DASA 1517

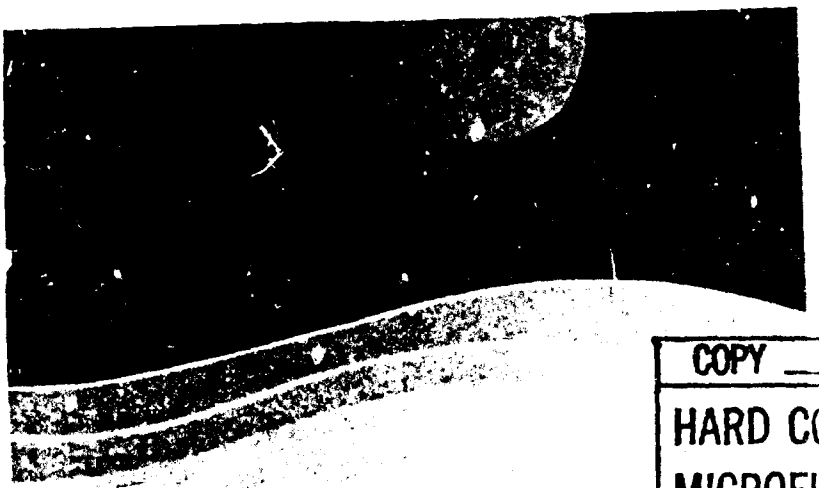

Project Springfield Report

E. F. Danielsen

July 1964

DEFENSE ATOMIC SUPPORT AGENCY
WASHINGTON, D.C. 20301

A NOTE ABOUT THE COVER

The painting which is reproduced on the cover was painted by the author in 1953. It depicts the troposphere, stratosphere, ionosphere, outer space, and cumulus and stratus cloud forms. The hydrological cycle, including a leaf form to symbolize evapotranspiration, and the stream flow of vortex motion are also depicted. It seemed appropriate to include this painting, for many of the ideas expressed verbally in the report are expressed graphically in the painting.

CLEARINGHOUSE FOR FEDERAL SCIENTIFIC AND TECHNICAL INFORMATION CFSTI
DOCUMENT MANAGEMENT BRANCH 410.11

LIMITATIONS IN REPRODUCTION QUALITY

ACCESSION # AD 607950

☐ 1. WE REGRET THAT LEGIBILITY OF THIS DOCUMENT IS IN PART UNSATISFACTORY. REPRODUCTION HAS BEEN MADE FROM BEST AVAILABLE COPY.

☐ 2. A PORTION OF THE ORIGINAL DOCUMENT CONTAINS FINE DETAIL WHICH MAY MAKE READING OF PHOTOCOPY DIFFICULT.

☐ 3. THE ORIGINAL DOCUMENT CONTAINS COLOR, BUT DISTRIBUTION COPIES ARE AVAILABLE IN BLACK-AND-WHITE REPRODUCTION ONLY.

☑ 4. THE INITIAL DISTRIBUTION COPIES CONTAIN COLOR WHICH WILL BE SHOWN IN BLACK-AND-WHITE WHEN IT IS NECESSARY TO REPRINT.

☐ 5. LIMITED SUPPLY ON HAND: WHEN EXHAUSTED, DOCUMENT WILL BE AVAILABLE IN MICROFICHE ONLY.

☐ 6. LIMITED SUPPLY ON HAND: WHEN EXHAUSTED DOCUMENT WILL NOT BE AVAILABLE.

☐ 7. DOCUMENT IS AVAILABLE IN MICROFICHE ONLY.

☐ 8. DOCUMENT AVAILABLE ON LOAN FROM CFSTI (TT DOCUMENTS ONLY).

☐ 9.

PROCESSOR: ca

TSL-107-10 64

DASA 1517

REPORT

on

PROJECT SPRINGFIELD

by

E. F. DANIELSEN

A report of work performed under Defense Atomic Support Agency Contract DA-49-146-XZ-079 with Isotopes, Incorporated, 123 Woodland Avenue, Westwood, New Jersey

15 July 1964

HEADQUARTERS, DEFENSE ATOMIC SUPPORT AGENCY

Washington, D. C. 20301

ABSTRACT

This report is concerned with the theory and confirmation of a stratospheric-tropospheric exchange which accompanies a folding of the tropopause. Air from the lower part of the cyclonic stratosphere is extruded to form a thin inclined layer in the troposphere. The SPRINGFIELD data prove that the extruded tropospheric layers contain radioactivity concentrations typical of the stratosphere. Concentrations exceeding the tropospheric by one or two orders of magnitude were measured aboard WB-50 and RB-57 aircraft on specially vectored flight paths. The sharp change in concentrations at the boundaries also confirms that the folding process is predominantly laminar, so it is appropriate to refer to the exchange as a transport rather than a diffusion process.

The agreement between the radioactivity and meteorological measurements is remarkable. Of particular value to the radiochemist and meteorologist is the high correlation between the concentrations of radioactivity and the potential vorticity. Since the latter can be determined from conventional radiosonde data, the three dimensional distribution of the former can be approximated. The distribution is not simple but the presence of the layers cannot be ignored in the fallout

prob'em. Each layer acts as a low altitude source for both wet and dry fallout.

The report contains as complete a description of the folding and transport process as is possible to date. Physical processes capable of mixing the radioactivity from the layers to the ground are also discussed, including their probable distribution with respect to the extruded layers.

PREFACE

Nature of Report.

This document is a special report on Project SPRINGFIELD, a research program funded by the Defense Atomic Support Agency and the Atomic Energy Commission. The U. S. Weather Bureau and several universities and industrial groups have cooperated in this project, the overall goal of which is to document and explain the spring fallout maximum by use of sampling aircraft and intensive collection and radiochemical analysis of rainfall. This report documents the first major undertaking of SPRINGFIELD: the verification of tropopause folding as a method of stratosphere -- troposphere exchange of fallout material.

A large store of information is now becoming available on the amount and location of radioactive debris injected into the stratosphere by nuclear weapons tests, and as a result, stratospheric transfer processes are beginning to be understood. The least understood facet of world-wide fallout has been the method or methods by which debris in the stratosphere enters the troposphere. That portion of Project SPRINGFIELD reported in this document is the experimental confirmation of the theory of tropopause folding and its importance in the transfer of radioactive debris.

ACKNOWLEDGEMENTS

Project SPRINGFIELD was made possible through the efforts of Dr. James Friend of Isotopes, Inc., Capt. Adrian Polk of the Defense Atomic Support Agency (DASA), Mr. Joshua Holland of the Atomic Energy Commission, Dr. Lester Machta and Mr. Robert List of the United States Weather Bureau (USWB), and Maj. Edward Nash of the Air Weather Service (AWS).

Financial support for the AWS sampling aircraft, the WB-50 and the RB-57, was supplied by DASA. Isotopes, Incorporated performed the chemical analyses of the aircraft radioactivity samples under a contract with DASA. The AEC and USWB supported the release and evaluation of extra radiosonde ascents and a few ozonesondes and gammasonde ascents. The latter were supplied by P. Gustafson, of the Argonne National Laboratory, who supervised the USWB releases. The arrangements were made by Mr. W. Hass of the USWB.

Special radar measurements and precipitation samples were taken in the Illinois Water Survey Network under the direction of Mr. Glenn Stout. Extra large precipitation collectors, designed to permit short term resolution of the radioactivity in precipitation, were built and set in the Illinois Network where they were manned by local volunteers.

Messrs. Larry Davis and Ray Booker obtained similar measurements at Pennsylvania State University, where an extra large rain gauge was placed in close proximity to a vertically oriented M33 Radar. Chemical analyses of the Illinois samples were made by Isotopes, Incorporated. Nuclear Science and Engineering Corporation analysed the Pennsylvania State samples. Financial support for these precipitation analyses came from the AEC.

The success or failure of the project depended upon the proper positioning of the aircraft during sampling. Major G. Corbell of the 9th Weather Reconnaissance Group, McClellan AFB, California, and Major Pair of the 1211th Test Squadron, Kirtland AFB, New Mexico, contributed much to formulating and organizing the flight plans and operational procedures. Major Pair even flew the first mission to test the feasibility of the RB-57 flight plans.

A similar willingness to extend themselves in the interest of the project was shown by Captain S. Martinenko, 55th Weather Reconnaissance Squadron, McClellan AFB, and Major T. Jensen, 1211th Test Squadron, who were Project Officers for the WB-50 and RB-57 aircraft. The project was directed by the author from the weather station at Pennsylvania State University. All decisions, flight plans and forecasts were telephoned to Captain Martinenko and Major Jensen, who, in turn, briefed the pilots and crews prior to each mission.

The author wishes to extend his appreciation to all who participated in Project SPRINGFIELD. Financial support of this project by the Defense Atomic Support Agency and Atomic Energy Commission is gratefully acknowledged.

TABLE OF CONTENTS

CHAPTER I

INTRODUCTION

Project SPRINGFIELD was organized to test a theory of mass transport from the stratosphere to the troposphere. As the tropopause folds, air from the stratosphere is drawn out to form a thin layer in the troposphere. If the exchange process is indeed a transport, the radioactivity and ozone concentrations of the stratospheric air should be approximately conserved during the layer formation. It follows from this that the distribution of radioactivity in the troposphere should be layered, with one or more distinct maxima and minima.

It is generally assumed that radioactivity enters the troposphere by diffusion -- either across the tropopause itself or along so-called "break lines" in the tropopause. It is further assumed that the troposphere is characterized by vigorous mixing which would dilute the concentration of any radioactivity or ozone once it entered the troposphere. From this conventional viewpoint, high concentrations of radioactivity would be found only in the stratosphere, some twelve to seventeen kilometers above sea level. In other words, the earth's surface should be insulated from the stratospheric radioactivity by the complete depth of the troposphere except for an occasional short circuit produced by the most intense cumulonimbus clouds.

The theory to be tested challenges both this viewpoint and its assumptions. It relates the folding process to cyclogenesis and predicts transport, almost to the earth's surface, when intense cyclones are formed. The transported radioactivity then acts as a low altitude source, of stratospheric intensity, for both wet and dry fallout. It is not difficult to imagine a variety of physical processes which could tap these sources. Several will be discussed in this report.

It would be misleading to leave the impression that testing the theory was the only purpose of Project SPRINGFIELD. It was its central purpose because of obvious implications to all aspects of the fallout problem. The project was also organized to coordinate air filter sampling with radar measurements and precipitation sampling. The relative importance of the numerous physical processes involved in wet fallout cannot be unscrambled without a coordinated measuring program. We may well find the data obtained in Project SPRINGFIELD insufficient for a solution to the wet fallout problem but it is certainly necessary.

The significance of programs of this type is also not restricted to the problem of world-wide fallout. Meteorologists are continually handicapped by their inability to trace an air parcel's movement through the three dimensional atmosphere. Many misconceptions have developed because the meteorologist is conditioned to view the motion two

dimensionally or quasi-two dimensionally. A few measurements made in the right place at the right time are worth all the effort required to make them.

CHAPTER II

THE THEORY AND IMPLICATIONS OF TROPOPAUSE FOLDING

Historical Background.

The concept of a folded tropopause appeared in the literature as early as 1937. Bjerknese and Palmer (1) considered a folded tropopause as the most logical interpretation of certain high level temperature and stability changes observed during the European Serial Ascents Program.

Sawyer, (2) in his 1946 study of the tropopause over Great Britain, also felt the data occasionally warranted this interpretation, but only occasionally. He attempted a Lagrangian analysis of the tropopause, i.e., an analysis of the changes following the three dimensional trajectories of the air parcels. However, his trajectories were computed from constant pressure charts and therefore offer little assurance that the computed trajectories correspond to the parcel's trajectories. The inability to trace and identify the same air parcels as they move with time limits his conclusions to an interpretation, perhaps correct, but not demonstrably correct.

In 1955, Reed (3) presented a rather convincing body of evidence to demonstrate that the tropopause actually does fold. Studying one case of tropopause folding over North America, he traced stratospheric air along descending trajectories into the troposphere. The trajectories were reconstructed from the steamlines on isentropic surfaces and

verified by the parcel's consistently large values of potential vorticity. His evidence, although internally consistent and physically meaningful, did not receive wide acceptance. It is easy, of course, to dismiss the results of one case study.

Support for the concept of tropopause folding, based on several cases, was presented by Reed and Danielsen (4) in 1959. They published a composite or mean cross section, oriented orthogonal to the flow, showing the distribution of potential vorticity in both the stratosphere and troposphere. Their mean cross section showed, as did Reed's study of 1955, that the large values of potential vorticity extended down and southward from the stratosphere into the troposphere. The tongue-like extension joined a tropospheric front at its lower limit and, except for its large value of potential vorticity, was indistinguishable from the tropospheric front. Since reasonable physical processes would require days or weeks to create these large values of potential vorticity from tropospheric air, the authors argued that its origin must be the stratosphere.

In the following year, Danielsen (5) published the results of a comprehensive tropopause study based on isentropic trajectories and the original radiosonde observations over North America. The original records processed in detail contained many thin layers or

laminae of high stability. Isentropic trajectories demonstrated stratospheric sources for many but not all of these laminae. The evidence implied that the folding process was frequent, and also implied that the folding produced thin layers which were eliminated from the processed radiosonde data -- unless two or more laminae merged to form a deeper lamina.

During the same year the author analysed in detail one case of tropopause folding to evaluate the mass transport from stratosphere to troposphere. This was found to be of the order of 10 grams per day per storm. The research was conducted at the Deutsche Wetter Dienst and the results were presented there at a seminar in October, 1959. The data and results were not published because strong objections were raised to the methods of trajectory computation. Since the answer depended directly on the reliability of the trajectories the author turned his attention to developing a more objective method of trajectory analysis.

An objective method was developed and published in 1961, Danielsen (6). When the method was applied to the case previously studied the former results were confirmed. But application of the method led to a better understanding of the folding process. In particular, it clarified the roles of the geostrophic and ageostrophic

velocity components. The important ageostrophic components are frequently too small to be measured, but their integrated effects can be determined through the trajectory analyses. Many of the concepts to be presented in the following chapters were derived from the application of this method.

In the Spring of 1960 the Weather Bureau conducted a special radioactivity sampling program to test the validity of the theory of tropopause folding. They flew B-57 aircraft in the vicinity of the tropopause over southwestern United States and obtained approximately 130 reliable filter samples between March and June.

In 1961, the author, with the assistance of several graduate students, determined the meteorological conditions appropriate to 126 samples. The number and locations of filter samples for any particular case were not sufficient to prove or disprove the theory. But it is possible to check on one aspect of the theory. As mentioned earlier, it was argued that the large values of potential vorticity had their origin in the stratosphere. If correct, this implied a positive correlation between the concentration of radioactivity and the potential vorticity.

The activity of several isotopes, such as Sr^{90}, Sr^{89}, W^{185}, and Be^{7}, were plotted using potential temperature and potential vorticity

as orthogonal coordinates. The results appear in a technical report by Danielsen, Bergman and Paulson (7) published in 1962. All of the samples extracted from air with a large potential vorticity had high Sr^{90}, W^{185} and Be^{7} activities and no measurable Sr^{89} activity. Since no measurable Sr^{89} activity should have remained from the tests which preceded the moratorium, the assumption was confirmed. On the other hand, high Sr^{89} activities, unambiguously attributed to the French Sahara test of February 13, 1960, were extracted from air with intermediate values of potential vorticity and within a restricted potential temperature range. These samples came from stable layers on the anticyclonic side of a jet, and it is now known that the activity was deposited in stable layers, of approximately the same potential temperature, on the anticyclonic side of the so-called "subtropical jet." This lends credence to the assumptions that potential temperature and potential vorticity are quasi-conservative atmospheric quantities.

In the chapters immediately following, both of these quantities will be defined and discussed. They are fundamental to all remaining discussions; therefore, the author included these chapters to assist the reader who may not find them familiar.

Potential Temperature. The potential temperature of an air parcel is derived from the first law of thermodynamics by assuming a

negligible heat transfer between the parcel and its environment. As the parcel's actual temperature changes by compression or expansion, its potential temperature remains constant. It is computed from Poisson's relation

$$\Theta = T \left(\frac{p_o}{p}\right)^k \qquad 1$$

where T and p are the actual temperature and pressure and Θ and p_o are the potential temperature and reference pressure. It is customary to choose 1000 mb, approximately surface pressure, for the reference so that Θ is the temperature of an air parcel compressed to sea level pressure. The exponent, k = .286, is the ratio of the gas constant to the specific heat at constant pressure.

In the atmosphere Θ increases with height; therefore, Θ can be used as a vertical coordinate instead of the height itself. If a parcel moves without any heat transfer, its Θ coordinate is invariant; conversely, a change in its Θ coordinate requires an energy transfer either by conduction, radiation, a phase change, or by mixing along the Θ gradient.

For radioactivity studies, the Θ coordinate has more physical significance than the usual height coordinate. If the radioactive particles are sufficiently small to remain in suspension, and this appears to be the case, at least for the products of air bursts, then they move

with the air molecules which suspend them. They are subject to the same physical constraints as the air parcels. The thermodynamic constraints can be interpreted from the Θ coordinate. Values of $\Theta > 400^{o}$ exist only in the stratosphere. This air can neither enter the troposphere nor reach the earth's surface without a diabatic process. Values between 300 and 400°K extend from the stratosphere into the troposphere. Air with a coordinate in this range may move from the stratosphere to the troposphere by an adiabatic transport; i.e., no diabatic process is necessary. At the lower limit of this range, between 320 and 300°K, the air may also be transported adiabatically directly to the earth's surface. What is implied here is the possibility of a direct transport from the lower stratosphere to the earth's surface. Dynamic constraints control the probability of this transport but we must recognize that thermodynamically it is possible.

From this viewpoint a stratospheric injection of radioactivity in the 300 to 320°K range may have as short a residence time as tropospheric injection, while the concentrations of radioactivity may be higher for the former than for the latter. The high latitude Russian explosions must be considered in this context. The usual distinction between a stratospheric and a tropospheric residence time may be misleading. From thermodynamic considerations the residence time should be a

function of the Θ coordinate. Dynamic constraints would be expected to modify but not negate the Θ dependence.

The above discussion indicates one advantage derived from the use of Θ coordinates. Another advantage is realized in the use of Θ surfaces for trajectory computations. The author, Danielsen (6), has shown that trajectories computed from the conventional constant pressure surfaces are subject to extremely large errors where vertical motions are large. Vertical motions in the atmosphere correlate positively with temperature advection and the latter correlates with a turning of both the wind and the pressure gradient with height. When these correlations exist, the curvatures of the parcel's trajectory are always more anticyclonic than the curvatures of a constant pressure trajectory. Thus, the parcel does not remain in vertical alignment with the constant pressure trajectory. The horizontal deviations are not negligible. Even in twelve hours they may become extremely large -- of the order of 1000 km . Also, on the pressure surface one usually cannot distinguish kinetic energy changes due to actual speed accelerations from changes due to the vertical advection of kinetic energy. The significance of speed accelerations will be illustrated later. Considering both sources of error, constant pressure trajectories are only reliable when vertical motions are negligibly small, but these cases are trivial.

Since the parcel's Θ coordinate is a slowly varying function of time, except in certain easily identified situations, both sources of error are eliminated by the use of Θ surfaces. The horizontal vector equation of motion yields two scalar equations, one governing the speed accelerations, the other the curvature accelerations. Speed changes are incorporated directly into the trajectory computation. The independent curvature equation can be used as a diagnostic equation to check on the reliability of the analyses. The method breaks down only when mixing occurs. It is important, therefore, to be able to detect the regions of mixing.

Potential Vorticity. Potential vorticity, the quantity Reed used as a tracer for stratospheric air, can also be used to detect mixing. It is a quasi-conservative scalar derived from the vector equation of motion, the continuity and energy equations, and is defined by

$$P \equiv a \nabla\Theta \cdot (\nabla \times V + 2\Omega) \qquad 2$$

where a is the specific volume, $\nabla\Theta$ is the three dimensional gradient of potential temperature and the term in parenthesis, the absolute vorticity, is the sum of the curl of the velocity and twice the angular velocity of the earth.

To an excellent approximation equation 2 can be reduced to

$$P_\Theta = -g \frac{\partial \Theta}{\partial p} (\zeta_\Theta + f) \qquad 3$$

where g is the acceleration of gravity, $-\frac{\partial \Theta}{\partial p}$ is a measure of the

stability of a parcel subject to a vertical displacement and $\mathcal{Z}_\Theta + f$ (the sum of the horizontal curl or vorticity measured on a Θ map and the vertical component, f , of the earth's vorticity) is a measure of the stability of a parcel subject to a horizontal displacement. P_Θ combines as a product of the two parcel stability criteria, namely, hydrostatic stability and inertial stability. If both terms are positive, a displaced parcel is forced back to its equilibrium position. If either is negative, the displacement is amplified and mixing develops.

As shown by Reed (3) and by Reed and Danielsen (4), the values of P_Θ in the stratosphere exceed the tropospheric values by one, two or three orders of magnitude. In the absence of mixing,

$$\frac{dP_\Theta}{dt} = -g\,(\mathcal{Z}_\Theta + f)\,\frac{\partial}{\partial p}\,\frac{(d\Theta)}{(dt)} \qquad 4$$

From this we can easily account for the creation of large stratospheric and low tropospheric values. Heating above and cooling below increases P_Θ , thus the heating source of the ozone layer generates large values in the stratosphere. Conversely, heating at the earth's surface generates low values and leads to vertical mixing in the troposphere. When cloud or moisture layers extend up to the tropopause the radiational cooling at their top accentuates both trends.

Excluding radiational cooling at cloud tops, $\frac{d\Theta}{dt}$ is a small quantity in the free atmosphere, i.e., above the friction layer and below the

ozone prediction layer. Therefore, P_θ tends to be conserved as does θ. For s riods both quantities approximate scalar invariants of the fluid and can be used as stationary Lagrangian coordinates.

This property permits one to trace and identify air of stratospheric properties. When the tropopause folds, tropospheric air with small values of P_θ folds over an extruded layer of stratospheric air with large values of P_θ. Since each parcel conserves its value of P_θ during the folding process, the air of stratospheric origin can be readily identified even after it is considered a part of the troposphere.

Tropopause Folding -- Two Dimensions. The process of tropopause folding and the trajectories of the extruded stratospheric air will now be traced out in detail through a series of two and three dimensional drawings. From the many individual cases studied by the author characteristic features have been abstracted to assist the reader in interpreting and appreciating the results of Project SPRINGFIELD.

Figure 1 includes a series of vertical cross sections with north to the right. In each cross section the stratospheric air has been toned gray. The lines sloping upward to the north in the troposphere, Figure 1a, and downward to the north in the stratosphere are lines of constant θ. Since the θ lines slope upward in the direction of colder temperatures both $\nabla_H \theta_p$ and $\nabla_H T_p$, the horizontal gradients of potential

temperature and actual temperature at constant pressure, are directed southward in the troposphere and northward in the stratosphere. The reversal in the horizontal temperature gradient coincides with the tropopause which slopes upward to the south. Note that θ increases southward along the tropopause. In Figure 1b and 1c the tropopause steepens and folds as the Θ lines change their spacing and in certain regions change their slope. Along the boundary between the stratospheric and tropospheric air Θ still increases from a low value in the north to a larger value in the south but the boundary no longer corresponds to a line of temperature gradient reversal. Also in the troposphere, a front has formed along a line extending southward from the fold. In the frontal zone the Θ surfaces have converged horizontally so the horizontal temperature gradient and the stability, $-\frac{\partial \Theta}{\partial p}$, of the tropospheric air are comparable to that of the stratospheric air within the fold. The similarity in horizontal temperature gradient and stability between the tropospheric frontal zone and the extruded stratospheric layer has misled the meteorologist to draw no distinction between them as shown in Figure 2. A conventional analysis would consider a tropospheric frontal zone extending up to a smoothed tropopause. Furthermore, the frontal boundaries are usually disconnected from the tropopause. Obviously, Figures 1c and 2 imply drastically different distributions of stratospheric air, radioactivity and

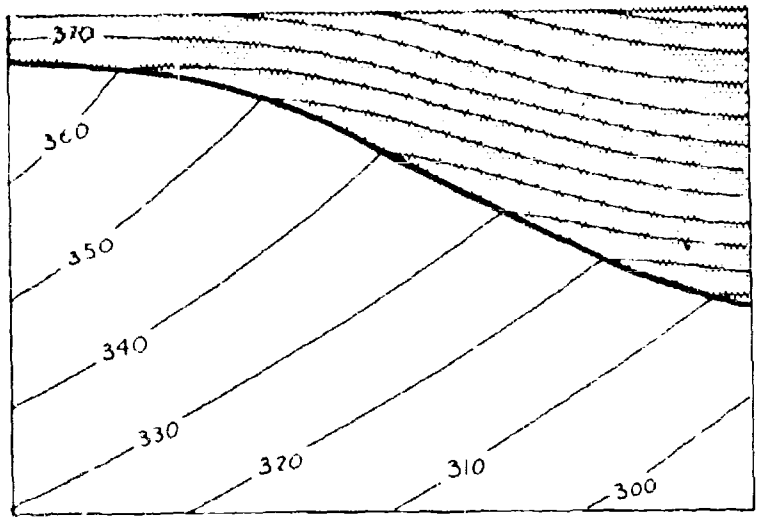

1a

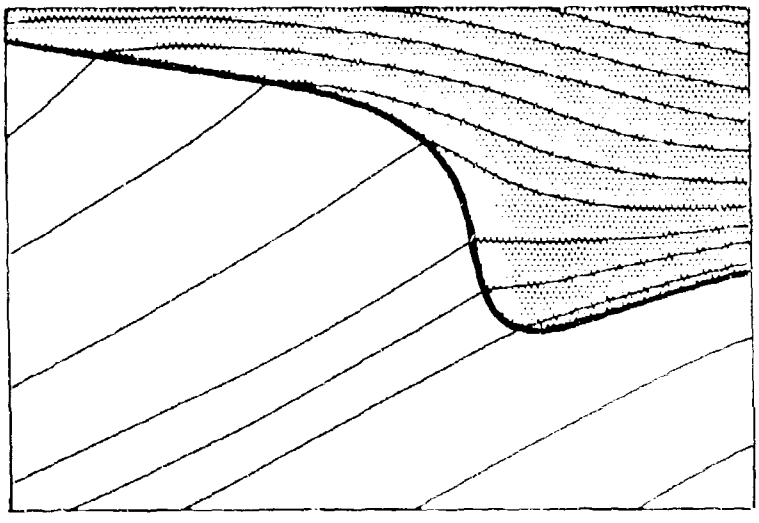

1b

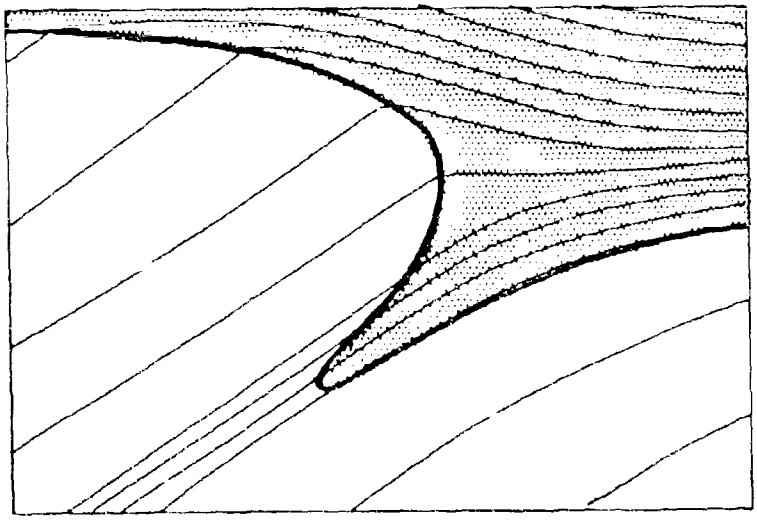

1c

Tropopause Folding and Tropospheric Frontogenesis in Vertical Cross Section

Figure 1

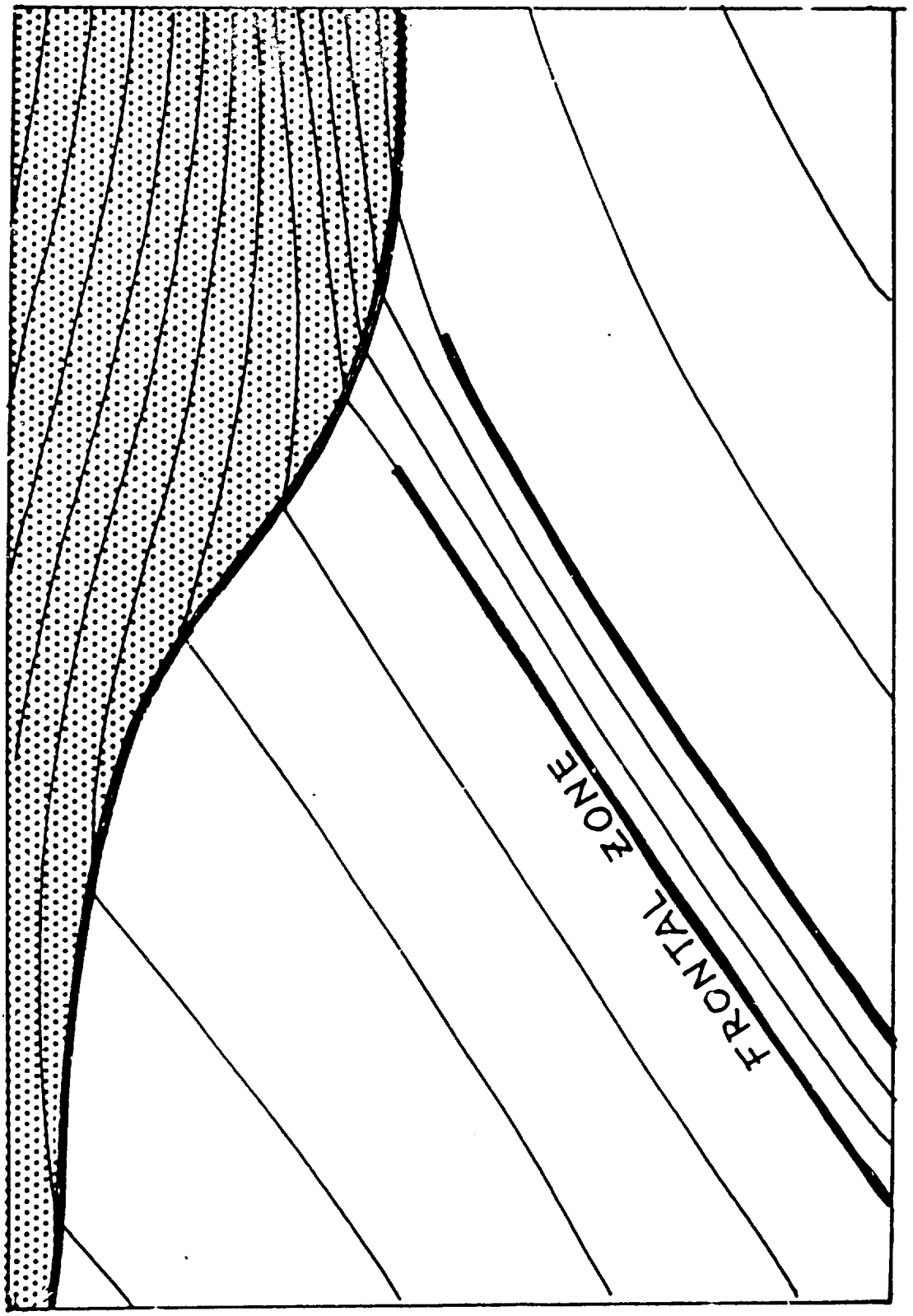

Figure 2 Conventional Analysis of Figure 1c

ozone. As will be shown, the tropospheric frontal zone and the extruded stratospheric layer can be distinguished by their distinctly different values of P_Θ.

Let us now consider the wind field and its changes as the tropopause folds and the tropospheric front forms. It is the wind field; specifically, the vorticity of the wind field, which will permit us to distinguish them. Figure 3a corresponds to Figure 1a. The additional set of dashed lines are isotachs, or lines of constant wind speed. In this case, they describe, in knots, the speed of the west wind, or u component of the wind. The black and white arrows represent the + and - v components of the wind. They have been drawn large to permit a visual comparison of their magnitudes but they are small compared to the u components. The significance of this distribution of v components will be discussed later. First we shall consider the u component of westerly flow. Note that the speed of the westerlies increases with height in the troposphere but decreases in the stratosphere. This follows from an assumption that the u component is in geostrophic balance. The speed is then directly proportional to the north-south pressure gradient and this increases with height in the troposphere because the air is warmer to the south. The decrease in the stratosphere is due to the reversal of the horizontal temperature gradient.

Figure 3a

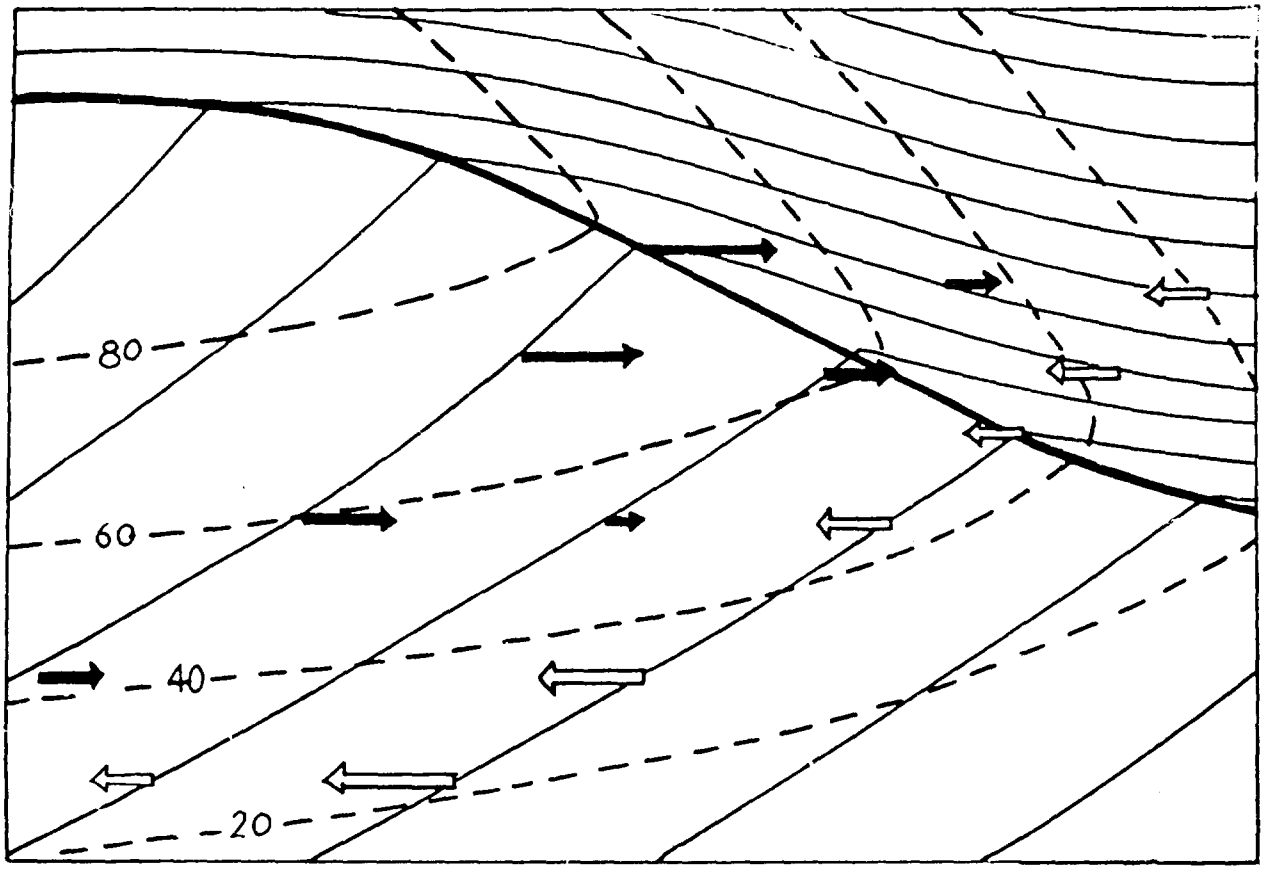

Convergence and Changes in Velocity
During Tropopause Folding

Figure 3b

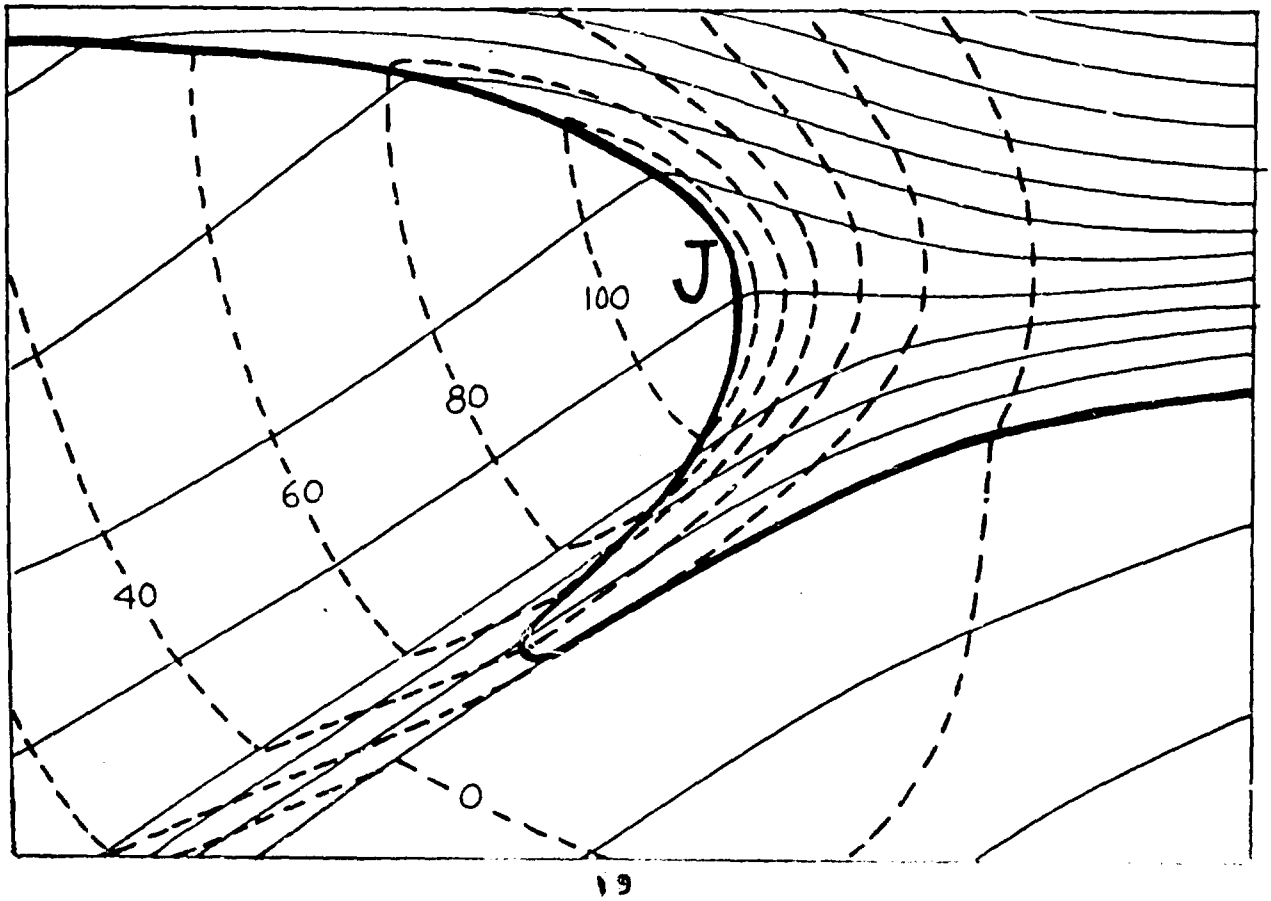

As the tropopause folds and a tropospheric front forms, the isotachs of the u component rotate toward the pattern in Figure 3b. Note that the distribution corresponds to Figure 1c. During the folding process speed accelerations and decelerations change the vorticity of the wind field. The question arises, "are these changes compatible with the assumption of adiabatic processes and the conservation of potential vorticity?"

To be compatible, several equations must be simultaneously satisfied. But before discussing these equations we must distinguish between two methods of analysing the relative vorticity. We can calculate the relative vorticity on surfaces of constant pressure or constant Θ. In both cases the horizontal winds are projected vertically to a horizontal surface; i.e., a pressure or Θ map, and then the horizontal derivatives are evaluated from the winds on the respective maps. Because the Θ surfaces slope much more than the pressure surfaces, the projected winds may differ considerably. In the troposphere the relative vorticity at constant p,

$$\zeta_p = \frac{\partial v}{\partial x_p} - \frac{\partial u}{\partial y_p}$$

may be positive while the vorticity at constant Θ ,

$$\zeta_\Theta = \frac{\partial v}{\partial x_\Theta} - \frac{\partial u}{\partial y_\Theta}$$

is usually negative. The difference is illustrated three dimensionally

in Figure 4, where the shear is positive, or cyclonic, at constant p and negative, or anticyclonic at constant θ. This difference is important because the two vorticities are governed by different equations and undergo change.. the opposite sign during frontogenesis.

When a front forms in the troposphere $\mathcal{L}_p$ increases, the stability increases, but $\mathcal{L}_\theta$ decreases. The equations that govern these changes under adiabatic processes are

$$\frac{d}{dt}(\mathcal{L}_p + f) = -(\mathcal{L}_p + f)\,\mathrm{div}\,V_p - K\cdot\nabla\omega \times \frac{\partial V}{\partial p} \qquad 5$$

$$\frac{d}{dt}\left(-\frac{\partial\theta}{\partial p}\right) = \left(-\frac{\partial\theta}{\partial p}\right)\mathrm{div}\,V_\theta \qquad 6$$

and

$$\frac{d}{dt}(\mathcal{L}_\theta + f) = -(\mathcal{L}_\theta + f)\,\mathrm{div}\,V_\theta \qquad 7$$

These equations show explicitly that this requires convergence (negative divergence) at constant p and divergence at constant θ. In equation 5 the right hand term, the so-called tilting term, includes a unit vertical vector, K, the total derivative of pressure, ω, and the vertical pressure derivative of the horizontal wind. This term is negligibly small initially but may dominate later.

Equations 6 and 7 combine to form the conservation of potential vorticity

$$\frac{d}{dt}\left[-\frac{\partial\theta}{\partial p}(\mathcal{L}_\theta + f)\right] = 0 \qquad 8$$

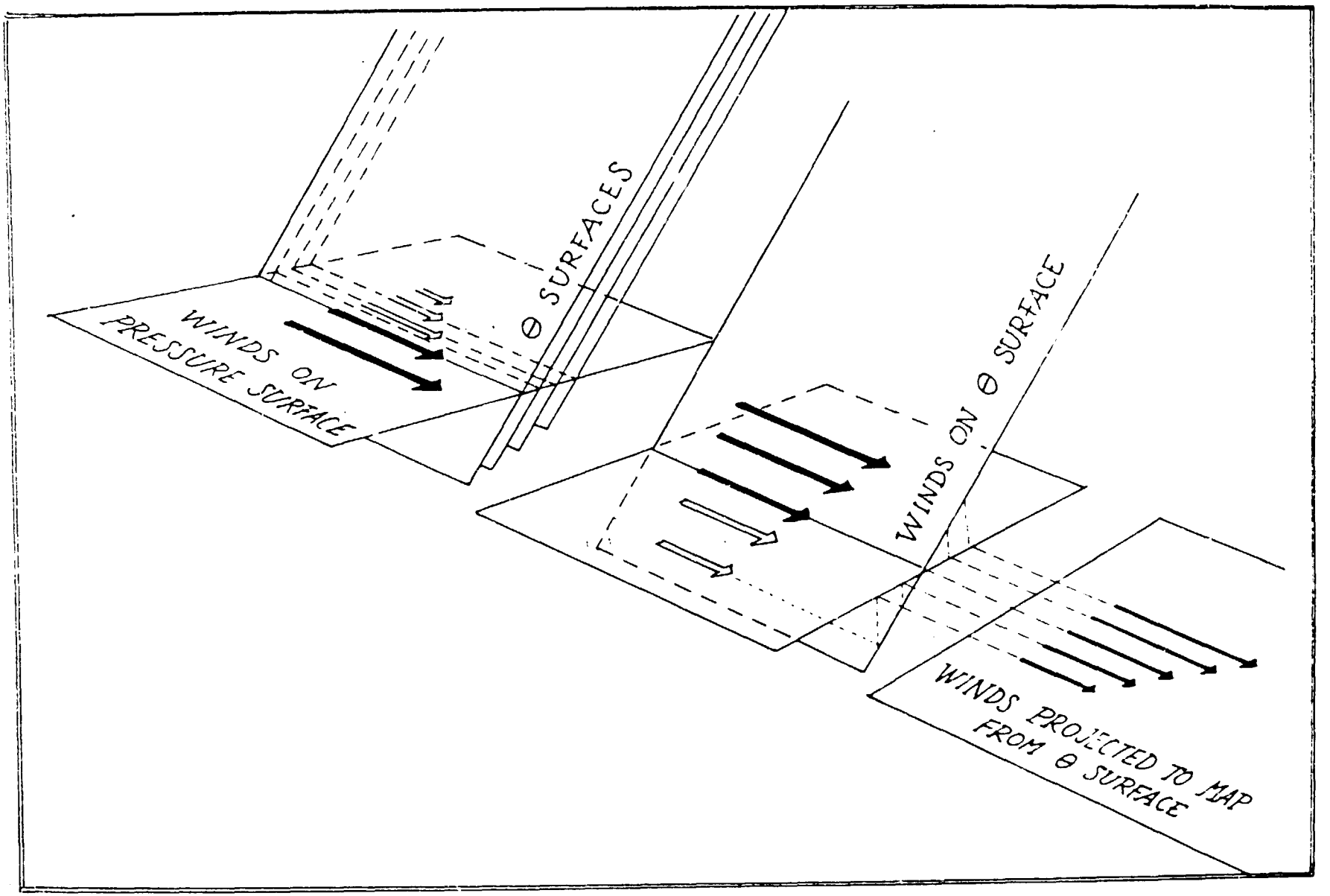

SHEAR VORTICITY OF HORIZONTAL WIND AT CONSTANT PRESSURE AND CONSTANT THETA

Figure 4

i.e., equation 8 is the same as equation 4 since we have assumed adiabatic processes. It is obvious, therefore, that the latter two changes, i.e., increasing stability and decreasing $\mathcal{L}_\Theta$, are compatible with the conservation of potential vorticity. All three changes are compatible when:

$$\text{div } V_p < 0$$

$$\text{div } V_\Theta > 0$$

Since the two divergencies are related by

$$\text{div } V_p = \text{div } V_\Theta + \frac{\partial V}{\partial \Theta} \cdot \nabla \Theta_p \qquad 9$$

the last term must be negative and dominant. Several authors have neglected this term in equation 9 by pointing out that where the vertical wind shear is geostrophic, $\frac{\partial V}{\partial \Theta}$ is orthogonal to $\nabla \Theta_p$ and the dot product is zero. However, when the wind shear is geostrophic, div V_p and div V_Θ are also probably small, so the argument is not applicable Certainly in tropospheric frontogenesis it must be the dominant term and it must be negative.

A velocity distribution that satisfies these requirements is shown in Figure 3a. If we neglect all variations in the x direction, normal to the cross section, then the v components determine the divergences. At constant p the positive v (black arrow) reverses to a negative v

(white arrow) in the positive y direction, thus there is convergence at constant p. At constant Θ the positive v component increases in magnitude in the y direction, thus there is divergence at constant Θ. It is also clear that $\frac{\partial V}{\partial \Theta}$ calculated from the v components -- the ageostrophic components -- points to the north while $\nabla \Theta_p$ points to the south: therefore, the last term of equation 9 is negative. The gradient of the u component, which is in geostrophic balance, contributes nothing to the last term.

It is also interesting that these conditions on div V_p, and div V_Θ require a large tilt in the axis of the convergence at constant p. It can be shown, when variations in x are neglected, that the tilt from the vertical must slightly exceed the tilt of the Θ surfaces. This checks out empirically because the tropospheric fronts contain approximately the same Θ surfaces from the ground to great heights.

If we examine the equations of motion we can recognize how the vorticity changes are produced. For no variation in the x direction,

$$\frac{du}{dt} = fv \qquad 10$$

$$\frac{d}{dt}\left(\frac{v^2}{2}\right) = -\frac{v}{\rho}\frac{\partial p}{\partial y} \qquad 11$$

where ρ is the density and $\frac{\partial p}{\partial y}$ is everywhere negative. The vorticities are computed from $-\frac{\partial u}{\partial y_p}$ and $-\frac{\partial u}{\partial y_\Theta}$, and we find from equation 10

that u increases where v is positive, (black arrow) and vice versa. Obviously, the u components increase where the arrows are black and decrease where the arrows are white with the result that the wind shear at constant pressure becomes strongly cyclonic. On the other hand, the u component increases more rapidly (or decreases less rapidly) to the north on the constant Θ surface. Thus, as the anticyclonic shear is increased, the relative vorticity becomes more negative.

It is also easy to see how the ageostrophic components, the black and white arrows, advect the Θ surfaces horizontally toward each other, thereby producing larger and larger stabilities.

The ageostrophic components in Figure 3a were not determined analytically nor numerically, but they are qualitatively and roughly quantitatively consistent with the speed, vorticity and stability changes between Figures 3a and 3b. They were included in Figure 3a to illustrate that all of the changes are compatible with the adiabatic assumption and the conservation of potential vorticity.

It should be pointed out that equation 9 can be used to eliminate div V_Θ from equation 6. Then this can be added to equation 5 to produce

$$\frac{d}{dt}\left[-\frac{\partial \Theta}{\partial p}\left(\zeta_\Theta + f\right)\right] = \left(\zeta_\Theta + f\right)\frac{\partial V}{\partial p} \cdot \nabla \Theta_p + \frac{\partial \Theta}{\partial p}\left(K \cdot \nabla\omega \times \frac{\partial V}{\partial p}\right) >> 0$$

The product in the brackets is not conserved, but on the contrary, increases rapidly in frontogenesis. Unfortunately there are many places

in the literature where this product with $\mathcal{L}_p$, not $\mathcal{L}_\theta$, is called the potential vorticity. The confusion has led some meteorologists to conclude that frontogenesis is incompatible with the conservation of potential vorticity. Also, it has contributed to a general mistrust of potential vorticity calculations.

We have seen a case where all changes are compatible and from these changes we can distinguish between the tropospheric frontal zone and the extended layer. As shown in Figure 3b, the increase in tropospheric stability requires a decrease in $\mathcal{L}_\theta$, i.e., it becomes more negative. On the other hand, $\mathcal{L}_\theta$ in the stratospheric air is initially positive and where the stability decreases, as for example just north of the jet, $\mathcal{L}_\theta$ becomes more positive. Therefore, when the stabilities are comparable,

$\mathcal{L}_\theta < 0$ characterizes the tropospheric air

$\mathcal{L}_\theta >> 0$ characterizes the stratospheric air

and in general

P_θ (in the layer) $>> P_\theta$ (in the tropospheric front).

This is consistent with the initial conditions where

P_θ (stratosphere) $>> P_\theta$ (troposphere).

Tropopause Folding - Three Dimensions. We have considered the folding process in only two dimensions to clarify the role of the

ageostrophic motions. Although these ageostrophic velocities are small, frequently too small to be measured, they produce the all important speed, stability and vorticity changes in both the stratospheric and tropospheric air.

To obtain a proper three dimensional picture of the folding we must also consider the geostrophic motion. It is, after all, the dominant motion and as we shall see, it initiates the folding and determines the form of the extruded layer. Figure 5 attempts to illustrate in three dimensions these two properties of the geostrophic flow. In the upper right you are looking down on a magenta colored tropopause which slopes upward to the southwest. The potential temperature increases along the tropopause from 300 to 340°K. The Θ = 320°K intersection is at the jet core where the geostrophic wind, shown by the long white vector, is from the northwest. On the horizontal surface, which represents a pressure surface, the winds decrease and the temperatures increase going both northeast and southwest from the jet. This is illustrated by the winds at A and B and the red isotherms.

To obtain the geostrophic winds at the tropopause we integrate from point A down to Θ = 300°K, i.e., we add the negative thermal wind vector (red) to the wind at point A. The resultant wind (black) is rotated toward the southwest . It then has a component which advects the low

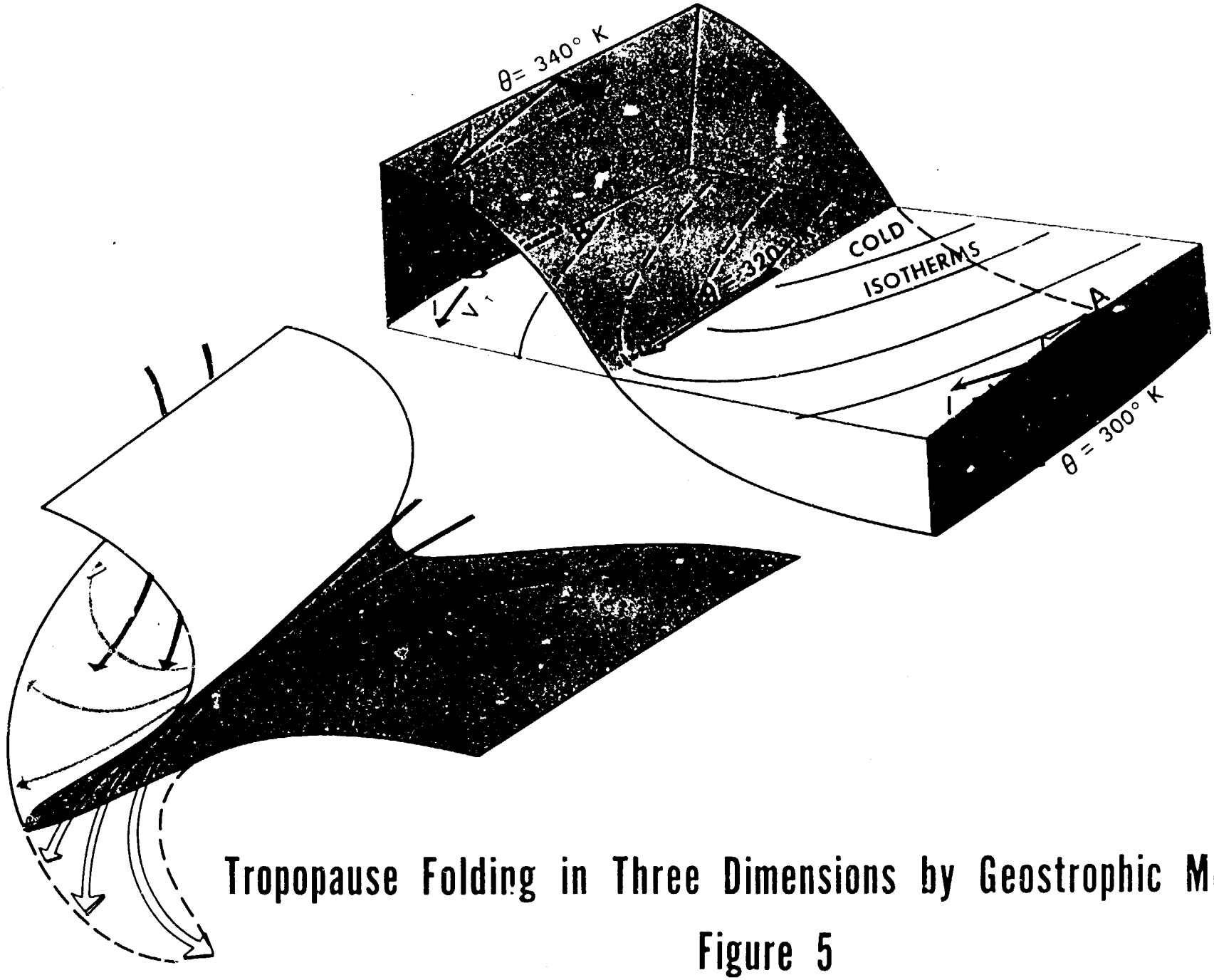

Tropopause Folding in Three Dimensions by Geostrophic Motions

Figure 5

tropopause southwest. At point B we add the thermal wind vector to obtain the tropopause wind at $\Theta = 340^{\circ}K$. Here we find the resultant vector is rotated toward the northeast. It has a component which advects the high tropopause northeast. Since the wind at $\Theta = 320^{\circ}K$ produces no advection we can see that the tropopause steepens relative to the jet core simply by geostrophic motions.

The steepening is a consequence of the thermal field which has this shape between a ridge and the next downstream trough. Thus, the tropopause should be steeper in the trough than in the ridge. East of the trough the thermal field reverses so the tropopause becomes less steep by geostrophic motions. If only geostrophic motions occurred, the process would be reversible -- tropopause steepening to the trough, flattening to the ridge. But vertical motions and the small ageostrophic components render the process irreversible. With the cold advection the northwest flow descends and the tropopause surface folds as shown in the lower left of Figure 5. The strong winds draw out the folded layer to a crescent shape as shown by the white flow arrows which extend from the shaded layer, and the dashed magenta outline. In other words, the folded layer (viewed from above) has a crescent shape, while in the vertical it appears as a thin layer inclined downward to the south. Since it is inclined, it intersects a pressure surface as a narrow zone approximately parallel to the wind. It has the horizontal temperature and wind

speed gradients characteristic of a tropospheric front, but as we saw, it has a much larger potential vorticity.

Trajectories in Extruded Air. We may now turn our attention to the three dimensional trajectories in the extruded stratospheric air as illustrated in Figure 6. The horizontal plane contains a surface map analysis appropriate to the extruded flow. The vertical plane is included to aid the illusion of three dimensional space.

Starting at the upper left, the trajectories descend and fan out. The deformations in the flow pattern are extremely large and very significant. A long thin rectangle parallel to the jet in the upper left is deformed to a long thin rectangle perpendicular to the flow along the leading edge of the extruded layer.

The deformations are related to the speed decelerations characteristic of the descending flow. To the right of the jet, facing downstream, the air is supergeostrophic. Because it is supergeostrophic, the air is decelerated and turned to the right. As it descends, it continues to enter a weaker and clockwise rotated geostrophic field. It therefore continues to be supergeostrophic and experiences further speed reductions and anticyclonic turnings. In extreme cases this trend continues until the air descends almost to the earth's surface where it forms the southeasterly flow around the surface anticyclone or high pressure area.

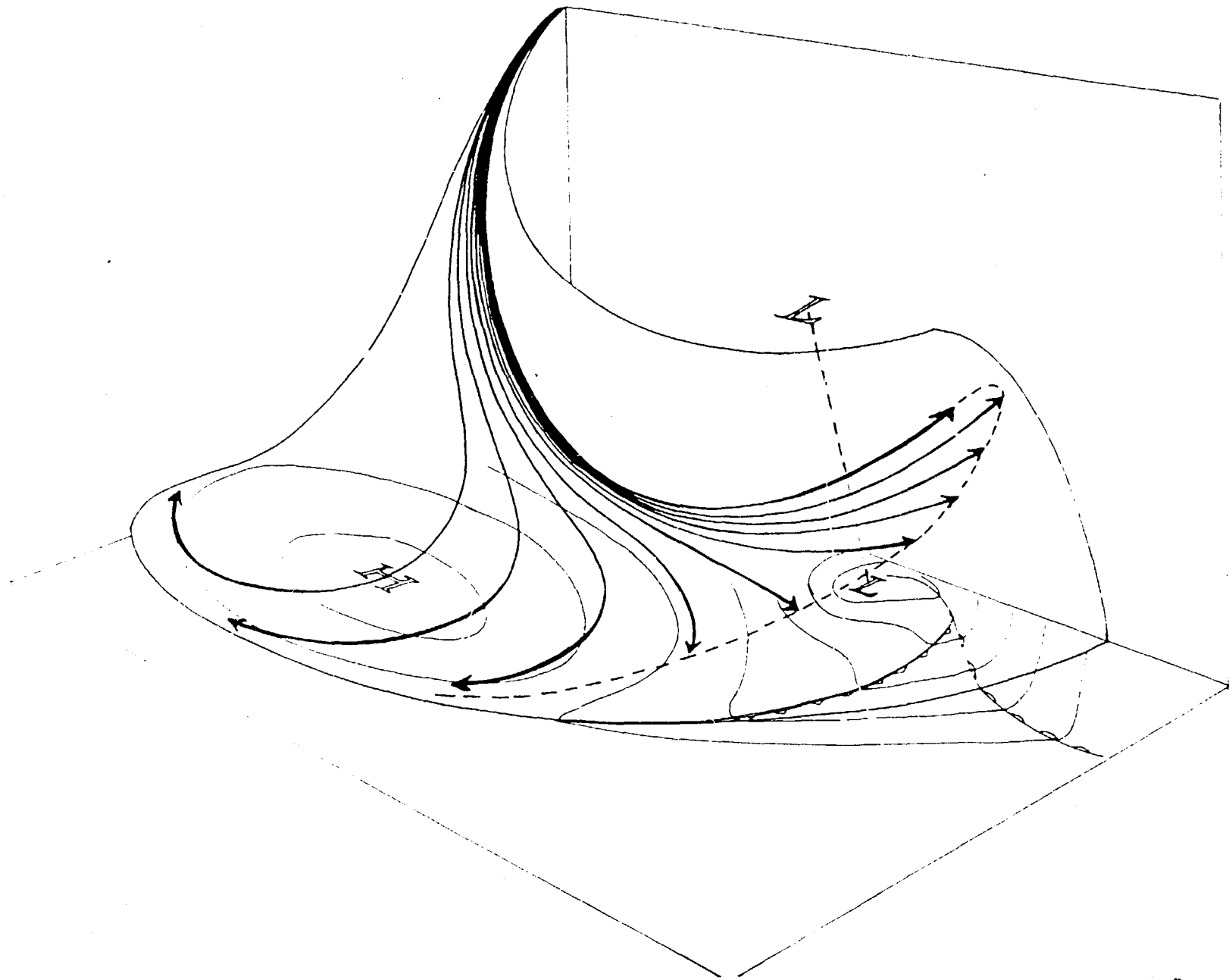

Figure 6 Trajectories of Extruded Stratospheric Air

From constant pressure analyses one would not suspect that the low level anticyclone is fed by descent from the upper troposphere or lower stratosphere. On the constant Θ analyses this descent and deformation is characteristic of every cyclogenetic process. The descent does not usually continue to the earth's surface as laminar flow. Turbulent eddies generated at the surface by rough terrain and/or surface heating penetrate and mix with the descending air. The mixing dilutes the radioactivity concentrations because the tropospheric air ascending in the eddies is virtually uncontaminated. As we shall see, the surface induced mixing may extend to depths of 10,000 and 15,000 feet. When this happens, the radioactivity concentrations are significantly reduced.

Dry Fallout. The descending, anticyclonical turning branch of the flow produces dry fallout at the ground several thousand kilometers to the south of the point where the folding is initiated. The resulting surface concentrations are a function of the initial lower stratospheric concentrations and the ratio of tropospheric to stratospheric air which is mixed by the turbulent eddies generated at the earth's surface. It should be noted here that the descending stratospheric air also transports high velocities downward, at the same time the eddies carry low velocities upward. Large vertical shears are produced which supply the energy to sustain or increase the mixing. In other words, low Richardson's

numbers are generated near the top of the mixing layer. The combination of the downward momentum transport and surface heating promotes vigorous mixing, strong gusty surface winds and dry fallout.

Wet Fallout. Returning now to Figure 6 and directing our attention to the central and left portions of the extruded flow we note that this air descends until it reaches the trough. After it passes the trough it ascends. The ascent may begin to the west of the surface front but continues well in advance of the front. At its leading edge the ascending dry, stable stratospheric air flows above ascending moist or saturated air. The high stability of the stratospheric layer suppresses vertical cloud development but the presence of the dry layer over saturated air is potentially unstable. As the ascent continues the latent heat released at the base of the layer by the condensing water vapor decreases the stability.

When the stability is reduced to a critical value, the cumulus clouds break through the layer and are then accelerated upward by strong bouyancy forces. A line of rain showers and thunderstorms quickly develops along the leading edge of the destabilized layer. As the cumulus clouds penetrate and break through the layer torroidal circulations entrain the stratospheric air into the growing cloud. If the radioactivity in the stratospheric air is attached to freezing or condensation

nuclei, the radioactivity will then enter the precipitation cycle. Since the stratospheric air is known to contain sulphate particles, Junge (8), Friend (9) and ice nuclei, Bigg (10) this mechanism may be quite probable. At present the process can only be inferred; it remains to be proven or disproven.

The destruction of the stratospheric layer along its leading edge is, however, not an inference. Trajectories in the stratospheric air consistently overshoot the leading edge -- where surface observations, radar measurements and satellite photographs confirm the presence of a line of cumulonimbus. All of the evidence fits the concept of a laminar-like transport toward the leading edge where entrainment in the developing cumulonimbus destroys all of the air's stratospheric characteristics.

The layers constitute a source for radioactivity -- a source with stratospheric concentrations but located several thousand feet below the stratosphere proper. If the tropopause did not fold and extrude these layers, cumuli would have to penetrate the stratosphere to entrain similar concentrations. In many cases this would require that the clouds attain elevations some 40 or 50 thousand feet above sea level. Furthermore, the air extruded in the layers comes from the cyclonic stratosphere where the potential vorticity is always large in magnitude, while the huge cumulonimbus which penetrates the stratosphere may entrain air from

the anticyclonic stratosphere where the potential vorticity may be as small as that of tropospheric air. The samples taken in 1960 by the RB-57's and some taken by the WU-2's for HASP showed very low concentrations of radioactivity in this region of the stratosphere while the samples taken in the cyclonic stratosphere always contained large concentrations. If we can generalize from the measurements made to date, cumulus penetration into stratosphere air is necessary but not a sufficient requirement for the entrainment of air rich in radioactivity, while cumulus penetration into air with a large potential vorticity may be both necessary and sufficient.

CHAPTER III

OPERATION OF PROJECT SPRINGFIELD

Flight and Sampling Requirements.

In most of the existing sampling programs the flight operations are kept simple. Flight tracks, altitudes and sampling procedures are determined and held constant. The data obtained is then interpreted statistically in terms of the mean distribution with latitude and altitude and the deviations from the mean.

For Project SPRINGFIELD this approach would be inappropriate. The samples had to be taken relative to the atmospheric structure wherever the structure happened to be. However, since a theoretical model was being tested we could prearrange an optimum set of sampling positions which could be held invariant relative to the structure. In this way the pilots and crews could concentrate on locating the structures and not worry about where or when to make a sample.

The sampling procedures were adjusted to take advantage of the asymmetry of the extruded layer. An aircraft flying perpendicular to the wind would observe rapid changes in wind, temperature and relative humidity as it crosses the short dimension of the structure. Obviously the perpendicular flight track would be most useful for detection of the layer. Conversely, a parallel flight track should produce slow changes.

and therefore be ideal for sampling. The orientation of the flight during sampling had to be considered because the filter paper required a twenty to thirty minute exposure. During this time thirty to sixty thousand cubic feet of air at standard pressure and temperature sweep through the filter. Thus, a filter paper represents an integrated line sample and only approximates a point sample when the variations along the line are small. It would be difficult to verify the theory if the sampling method smoothed out the variations.

The planes were first sent to an initial point, or I. P., which was a TACAN station (a radio aid to air navigation) located near the center of a low or trough in the wind field. From this point they began their search at assigned altitudes and radial flight paths. Two WB-50's separated by 2000 feet were assigned altitudes below the lowest tropopause which would usually be reported at or near I. P. Thus all of the WB-50's samples would be considered tropospheric by the usual meteorological criteria.

All stratospheric sampling was left to the RB-57's. Fortunately, their sampling positions could be determined relative to the core of the jet stream. While maintaining a flight track between two TACAN stations the pilot could detect the core by monitoring the drift angle. Starting from the I. P. on the cyclonic side of the jet, the drift angle would increase rapidly to a maximum at the core and then decrease less rapidly

on the anticyclonic side. On many of the flights two jet streams were detected. Whenever this occurred, the jet closest to the I. P. served as the reference point for the first set of samples. When both wing tip samplers had been exposed, the pilot returned to Kirtland Air Force Base where the exposed papers were removed and replaced. Then he returned to make a second set of samples. On the second flight he sampled relative to the second jet, if two were detected, otherwise he returned to his previously located single jet and sampled at higher altitudes.

The locations of the RB-57 samples are shown in Figure 7. Note that if only one jet were detected, the two aircraft would take 8 samples -- 5 from the cyclonic stratosphere. The extruded air, which presumably the WB-50's would encounter and sample, has its origin in the cyclonic stratosphere and consequently should bear a close resemblance to the air north of the jet. The lowest samples on the cyclonic side were positioned to approximate the same potential temperature range as the layer. On the anticyclonic side one or two tropospheric samples were taken above the WB-50 samples to see if the activity in the layer actually represented a maximum in the vertical profile. Each filter paper was exposed for 15 minutes along a heading perpendicular to the flight track. In most cases, this means that the samples were taken either up or down wind and appear as a dot on the cross sections to be presented.

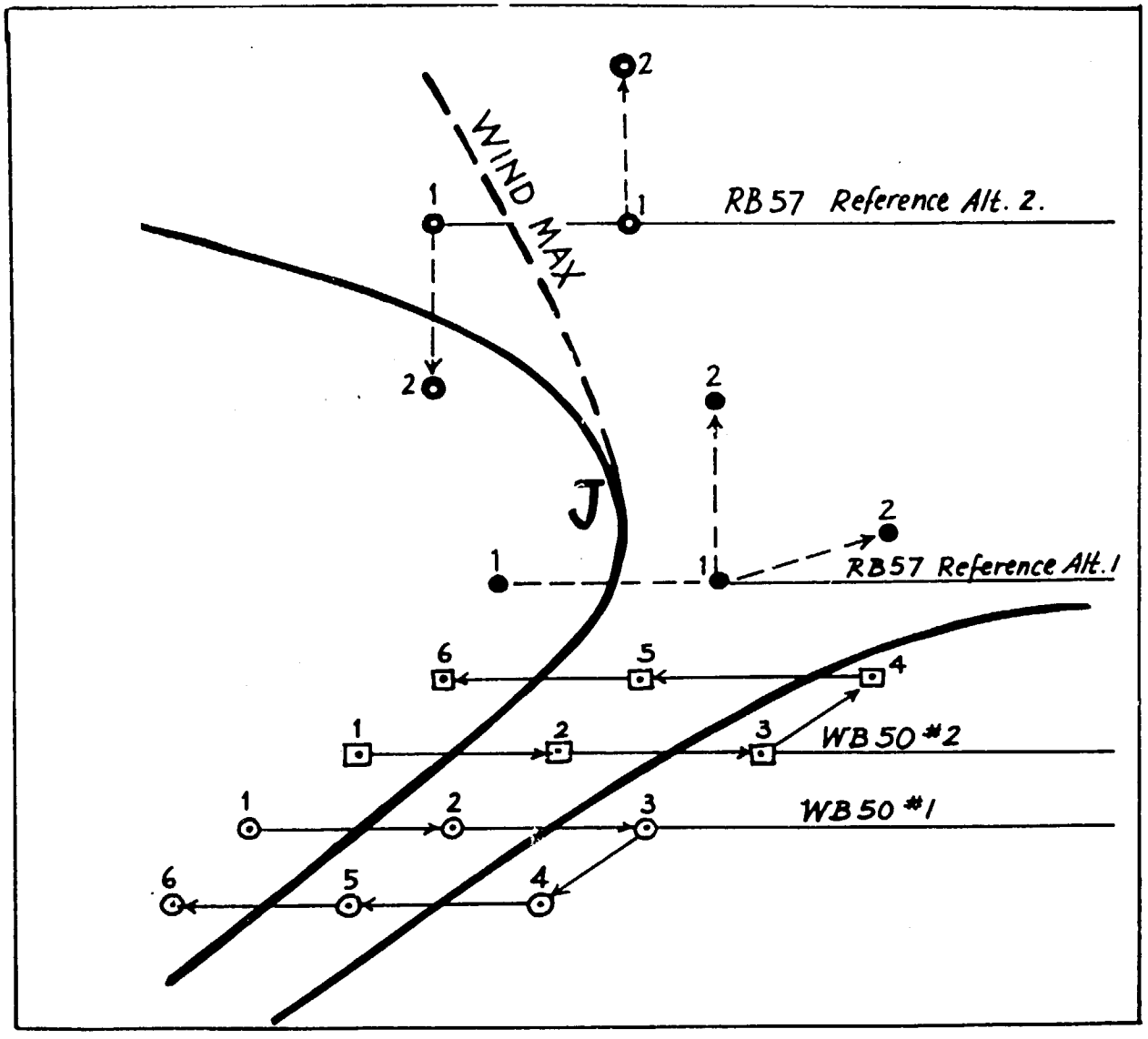

Flight and sampling Plans for WB50 and RB57 Aircraft

Figure 7

The weather observer aboard each WB-50 began recording the wind, temperature and dew point when he reached the I. P. By studying this record in flight he decided when and where the plane traversed a layer. He looked for a simultaneous rapid increase in temperature and wind speed followed by a slower increase in temperature and a decrease in wind speed. Ambiguities arose when multiple layers were detected -- some extremely narrow -- and when one of the criteria was not met.

In any event, he had to make a decision about the limits of the layer and then take three samples: one outside on the warm side of the layer, one inside, and one outside on the cold side of the layer. After completing these three samples the upper aircraft, #2, ascended to another assigned altitude while the lower aircraft, #1, descended. Once again they had to locate the layer and take three more samples each.

On the first flights the ambiguities produced some disappointments when certain points were not sampled but through experience the objectives and methods were clarified. Also the correspondence between the temperatures measured by the WB-50's and the radiosondes was so close that certain temperature ranges could be assigned for each sample and thereby reduce the uncertainty in sampling location.

Continuous Radioactivity Records. Each of the WB-50's is equipped to record the counting rate of a Geiger counter which faces a continuously

exposed filter paper. If the accumulated disintegrations of the debris exceeds the background count, the distribution of radioactivity can be observed in detail simply by traversing the layers.

To calibrate the accumulated counting rate to the activity in the air, we must differentiate the recorded trace and then determine an adjustment for the flow rate. However, since we are more concerned with relative rather than absolute concentrations of radioactivity, we can determine this at a glance by comparing slopes.

All traces shown in this report have been smoothed to eliminate the small amplitude, high frequency statistical fluctuations in the counting rate. The smoothed curve should always have a positive slope unless the decay rate exceeds the accumulation. In some cases negative or almost constant slopes were observed. These are caused by the rapid decay of radon daughter products and can be identified with cumulus convection currents ascending from the ground.

CHAPTER IV

RESULTS AND DISCUSSION OF SAMPLING FLIGHTS

General Flight Data.

A brief summary of all missions flown during Project SPRINGFIELD is presented in the following table. The range in altitude and range in β activities have been tabulated separately for the WB-50 and RB-57 aircraft. The lowest and highest activities represent only the range; they do not correspond to the lowest and highest altitudes. In some cases the lowest altitude sample had the highest activity.

Missions 8, 13, 15 and 16 were flown to check on the activities when no extruded layers were forecasted. In mission 7 the WB-50's could not penetrate the layer because it moved north of the Canadian border.

			WB-50		RB-57	
Mission	Date	Area	Altitudes (1000 ft)	β Activity (dpm/SCF)	Altitudes (1000 ft)	β Activity (dpm/SCF)
1	4/10/63	Utah	18-27	2-15	31-41	2-197
2	4/17/63	Nevada			27-39	8-265
3	4/18/63	Colorado	27	2-156	28-40	10-620
4	4/21/63	Nevada - Arizona	19-26	1-92	28-41	4-215
5	4/22/63	Utah - New Mexico	21-29	2-41	32-44	4-214
6	4/23/63	Michigan - Ohio	12-22	1-26	29-40	2-201

Mission	Date	Area	WB-50 Altitudes (1000 ft)	WB-50 β Activity (dpm, SCF)	RB-57 Altitudes (1000 ft)	RB-57 β Activity (dpm, SCF)
7	5/2/63	Wyoming-Montana	20-27	0.4-8	32-42	5-139
8	5/3/63	Illinois-Calif.	20-26	0.5-6	30-40	2-49
9	5/6/63	Texas			32-42	9-144
10	5/7/63	Off Oregon Coast	18-26	0.0-27		
10	5/7/63	Missouri			35-44	2-70
11	5/8/63	Washington-Idaho	19-28	0.4-65	33-43	4-170
12	5/9/63	Colorado			33-35	3-4
13	5/21/63	Calif-Minn-Ill.	17-19	0.5-8.0		
14	5/22/63	Ohio-New York-Ohio	15-25	3-25	29-35	4-171
15	5/23/63	Ill-Calif	16	0.7-5		
16	5/24/63	Ill-Calif	18	0.8-4		
17	5/29/63	Arizona			26-41	1-51
18	5/30/63	Utah			32-38	5-156
19	5/31/63	Texas-Oklahoma			32-43	5-179

Flight Data from Several Missions.

Analyses of the SPRINGFIELD data are still in progress. Data from several of the more interesting missions will be presented here

with the reservation that some features of the analyses may require modification when the isentropic charts and isentropic trajectories have been completed.

Each mission began at 1800 Z when the planes left the I. P. The missions were usually completed at 0100 or 0200 Z of the following day. With few exceptions, the maps and cross sections included here were drawn from the 0000 Z data. The maps, which will include the surface and either a 300 or 500 mb analyses, are included for reference only. They will not be separately discussed. The upper level maps contain a contour analysis and a few winds. The latter are plotted in the vicinity of the flight track which is a heavy dashed line beginning at the I. P.

Mission of April 18 - 19. The planes, two WB-50's and two RB-57's, were sent to an I. P. in southwestern Wyoming. From there they were to fly southeast, approximately perpendicular to the wind, as shown in Figure 8b. A clearance to cross the air lanes was delayed because of clouds and snow showers. The delay caused the WB-50 which had been assigned the lower altitude to abort the mission. Just as the pilot of the upper WB-50 was about to turn back, the plane broke into the clear. He then proceeded with the first portion of his mission.

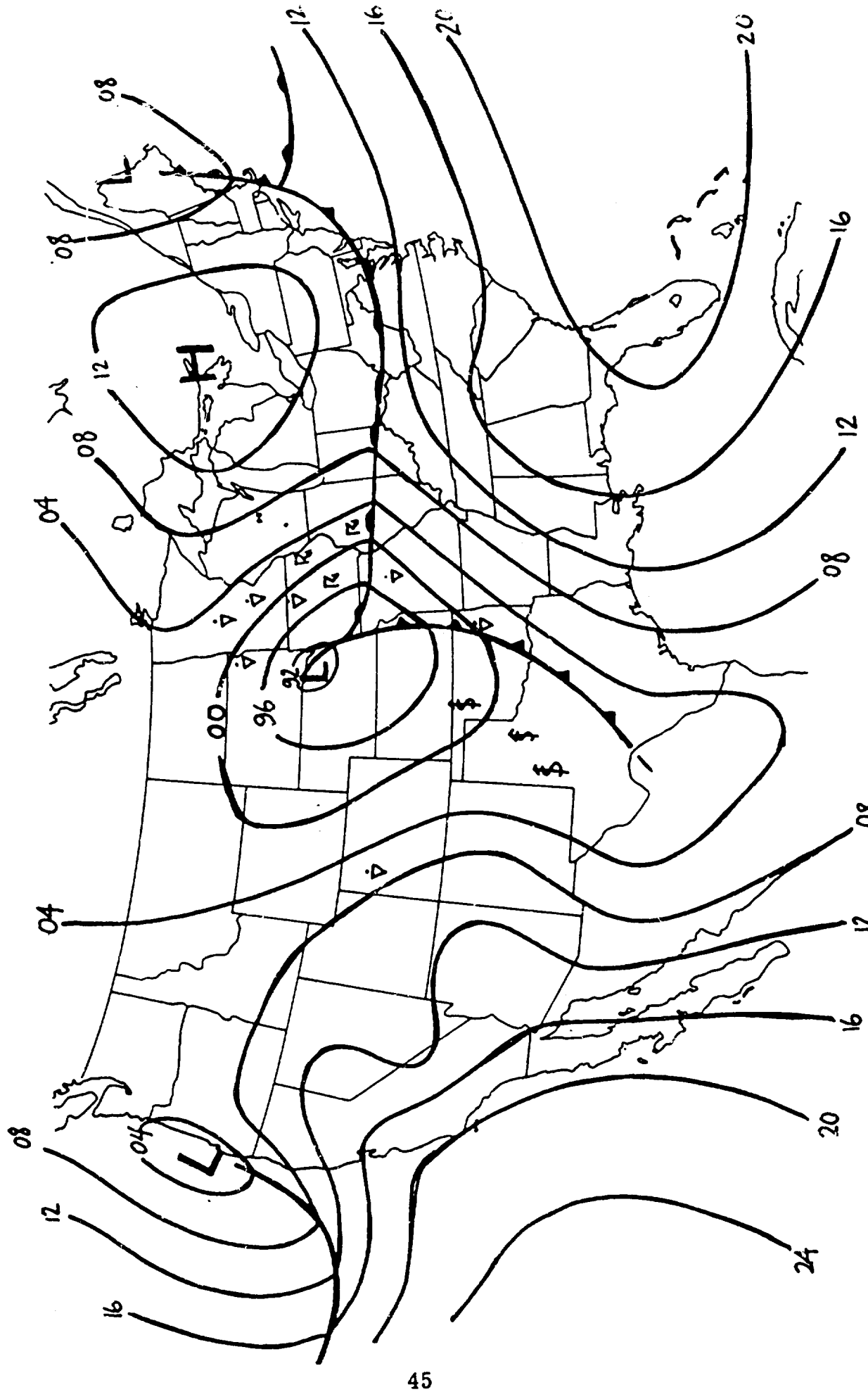

Figure 8a Surface Map-April 19,0000z,1963.

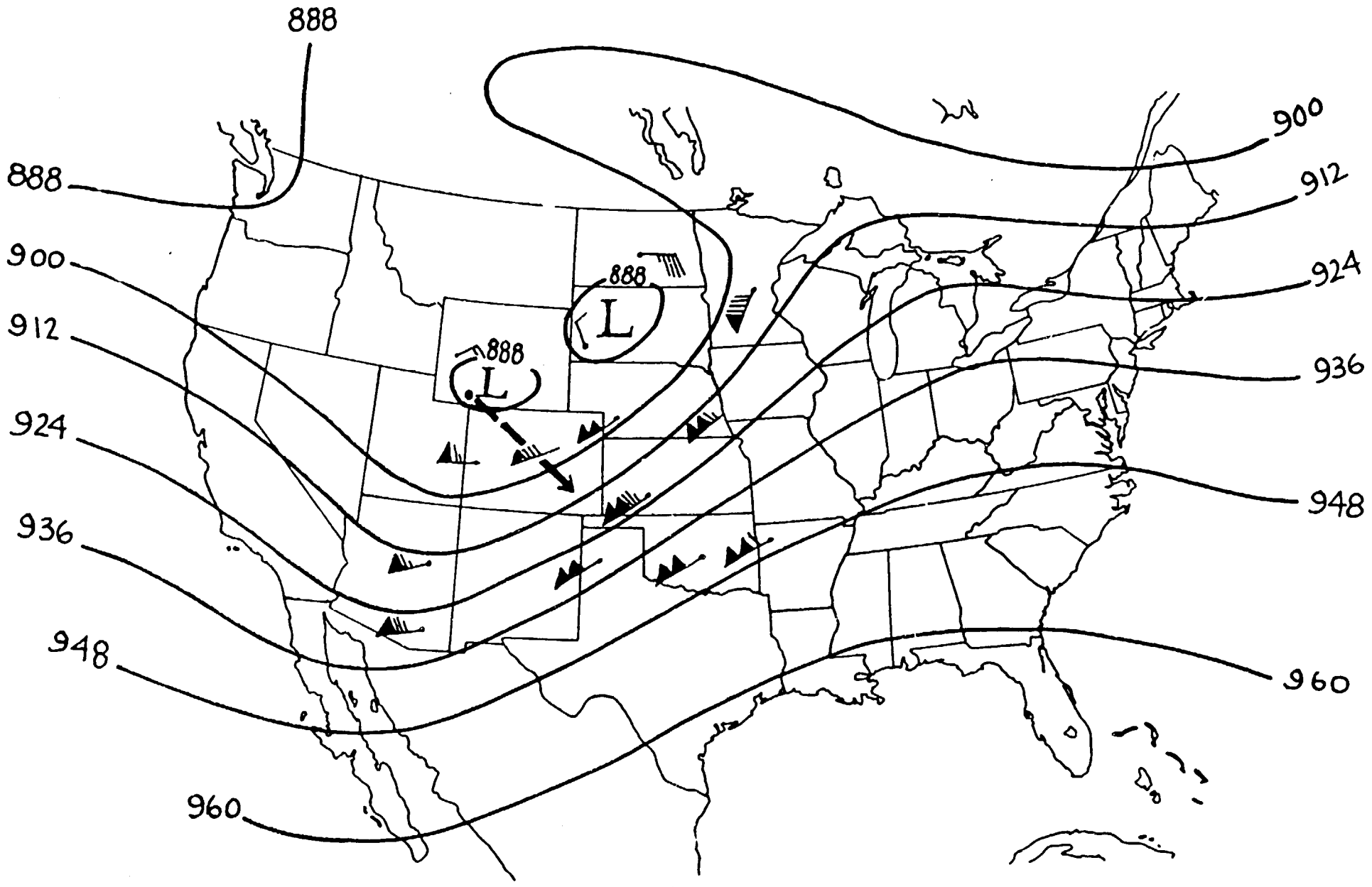

Figure 8b 300mb-April 19,0000z,1963.

The flight path of the upper aircraft, starting at 23,000 feet near Lander, is the purple line in Figure 9. To remain above cumulonimbus clouds, which were penetrating the dry stable layer, the pilot had to take the plane to 25,800 feet, then 27,000 feet. This altitude was maintained for the remainder of the mission.

The stable layer is easily distinguished by the closely spaced lines drawn at an interval of $2^{o}K$. Superimposed on the black Θ lines are red isotachs drawn at a 10 kt interval. To the left, where the isotachs are negative, the winds are from the northeast. The high wind speeds are all from the southwest and include three jets, each labeled with a red J.

As the plane traversed the stable layer the wind speed increased from 30 to 100 kt, the temperature rose from -48 to $-24^{o}C$, and the radioactivity counting rate on the continuously exposed filter paper increased from 1300 to 4000 cpm. These dramatic and synchronized changes are illustrated in Figure 10 by a medium width dashed line, a thin continuous line and a broad continucus linc.

Because the counting rate is proportional to the accumulated radioactivity, the slope is proportional to the disintegration rate per unit mass of air. The latter shall be called the "activity" and expressed in disintegrations per minute per standard cubic foot of air. Note that

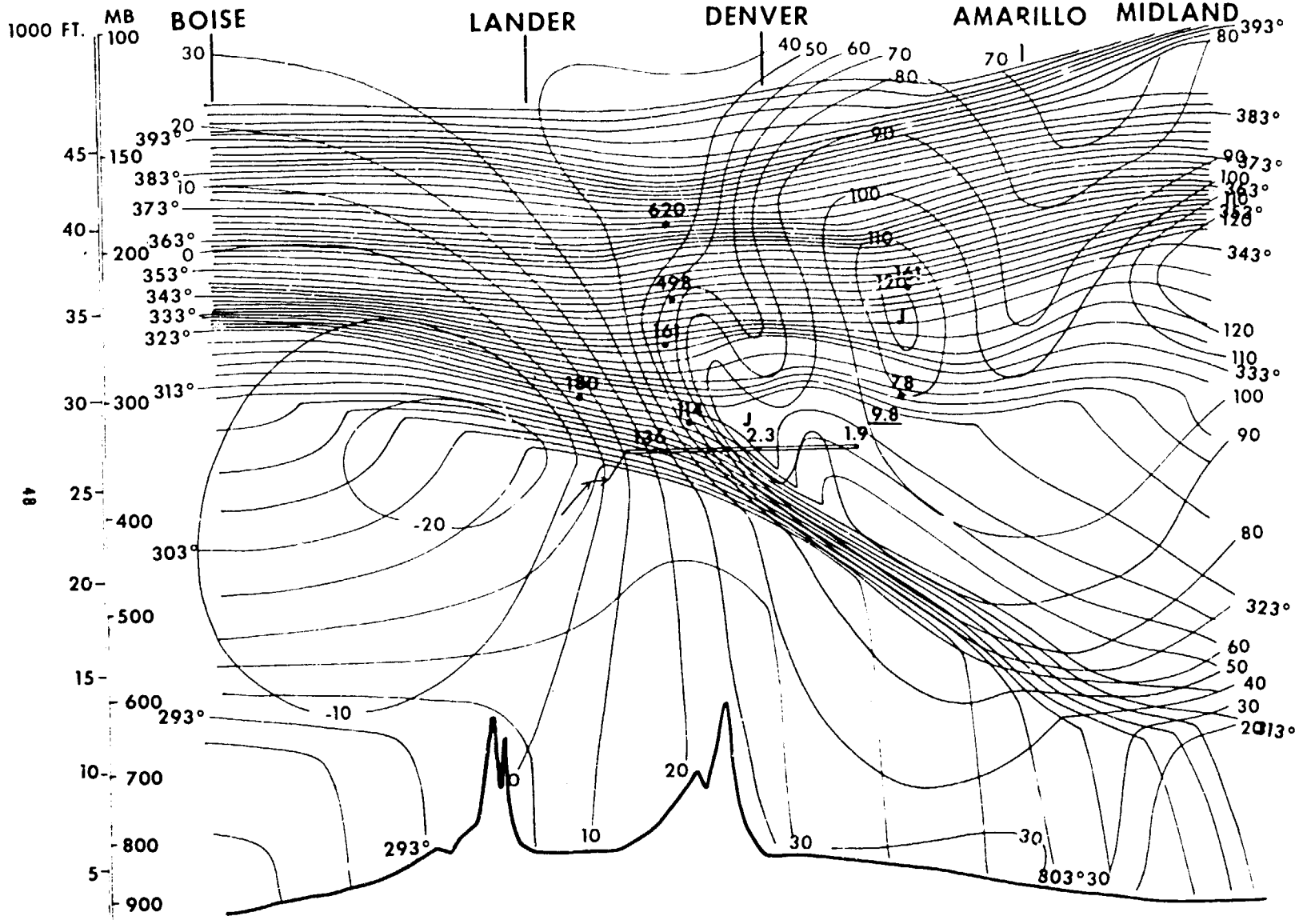

Figure 9 Vertical Cross Section for April 19, 1963, 0000z. Flight Path of WB 50 and Total β Activity of Filter Samples in Purple. Potential Temperature Analysis in Black - Isotach Analysis in Red.

Figure 10

Flight Data for WB50, April 18-19, 1963.

Altitude 23-27 thousand feet.

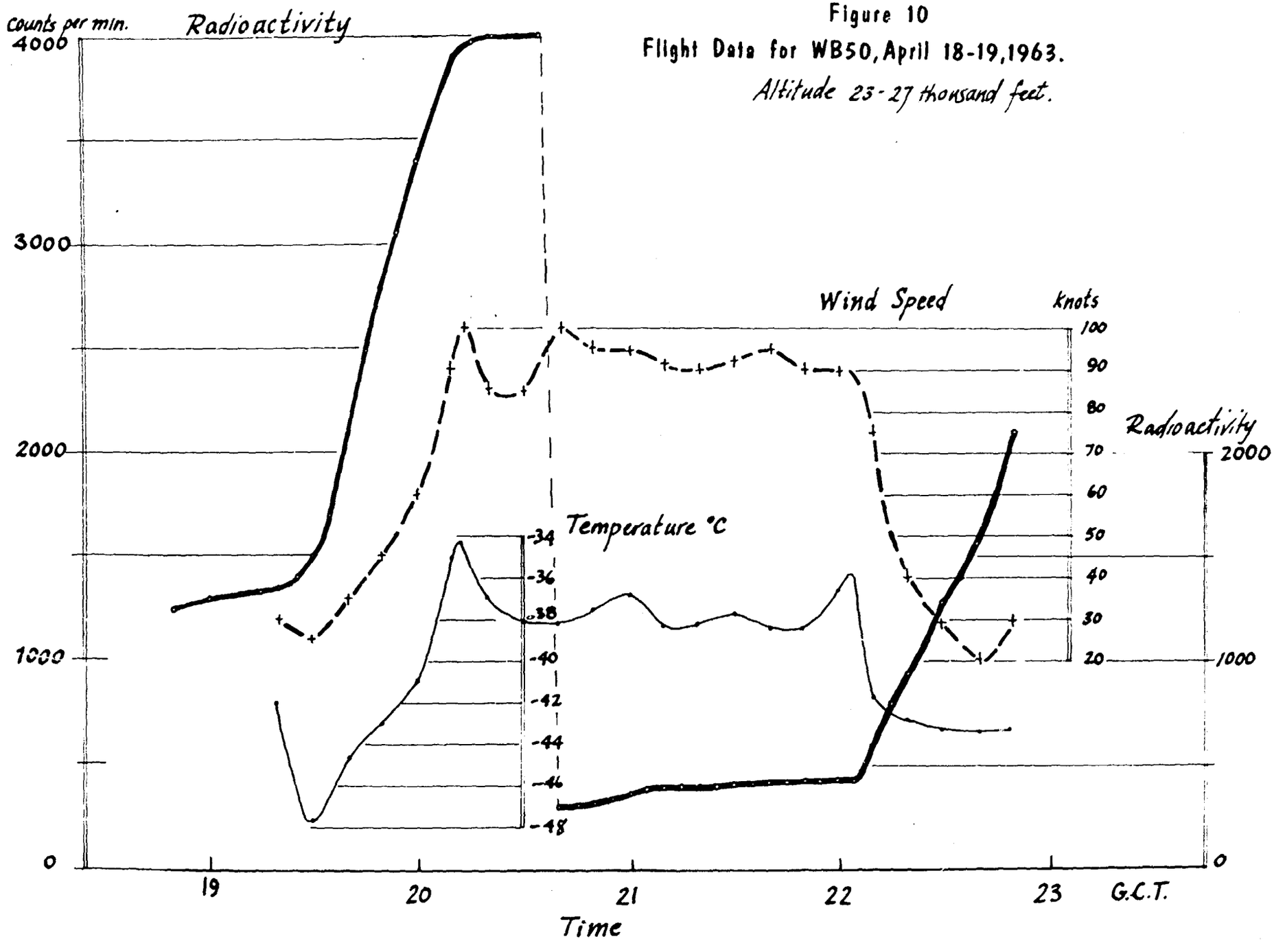

as the plane passed the warm boundary of the layer the wind speed and temperature decreased and so did the slope of the counting rate trace. The latter implies a rapid change from a high to low activity. Returning to Figure 9, we find this change verified by the β activities of three discrete filter samples taken by the WB-50 aircraft. In the stable layer the activity was 138 dpm/SCF while outside the layer the values were 2.3 and 1.9 dpm/SCF.

It is also worth noting that the change in slope was abrupt which implies negligible diffusion or mixing at the edge of the layer. The small difference between the two low activity samples -- the ones taken just outside the layer -- also supports this implication.

We also find that the activities were consistently high for the RB-57 samples taken on the cyclonic side of the jet. These activities were 114 and 180 dpm/SCF at $\Theta = 320^{o}K$, 161 dpm/SCF at $\Theta = 335^{o}K$, 498 dpm/SCF at $\Theta = 347^{o}K$, and 620 dpm/SCF at $\Theta = 371^{o}K$. Another interesting activity was the 78 dpm/SCF located beneath the central jet. This sample was taken from air which would be considered tropospheric by the conventional criteria. This sample shall be referred to later in the discussion of the potential vorticity.

The continuous counting rate and the discrete filter samples leave little doubt that the air in the stable layer at 27,000 feet is

stratospheric. We have no proof that the stratospheric air extends to lower elevations but we shall now look at evidence which suggests that it does.

Figures 11, 12, and 13 are the distributions of stability, absolute vorticity and their product, the potential vorticity. The calculations of stability and relative vorticity were made from the potential temperature and isotach analyses by finite differencing, i.e.,

$$-\frac{\partial \Theta}{\partial p} \simeq -\frac{2^{\circ}K}{\Delta p}$$

$$\zeta_{\Theta} = \frac{V}{R_{\Theta}} + \frac{\partial V}{\partial n_{\Theta}} \simeq \frac{\partial V}{\partial n_{\Theta}} \simeq \frac{10\ Kt}{\Delta n_{\Theta}}$$

where V is the wind speed, R_{Θ} is the radius of curvature of the streamlines on the Θ surface and n is the horizontal distance, positive to the right. The radii of curvature are large for most points in the plane of the cross section except near the center of the low. Therefore, on the cyclonic side of the northern jet the positive relative vorticities are underestimated while elsewhere the approximation is good. The occurrence of the three quantities depends primarily on the representativeness of the analyses. This is difficult to assess. The smaller scale features may not be representative but the large features can not be significantly altered.

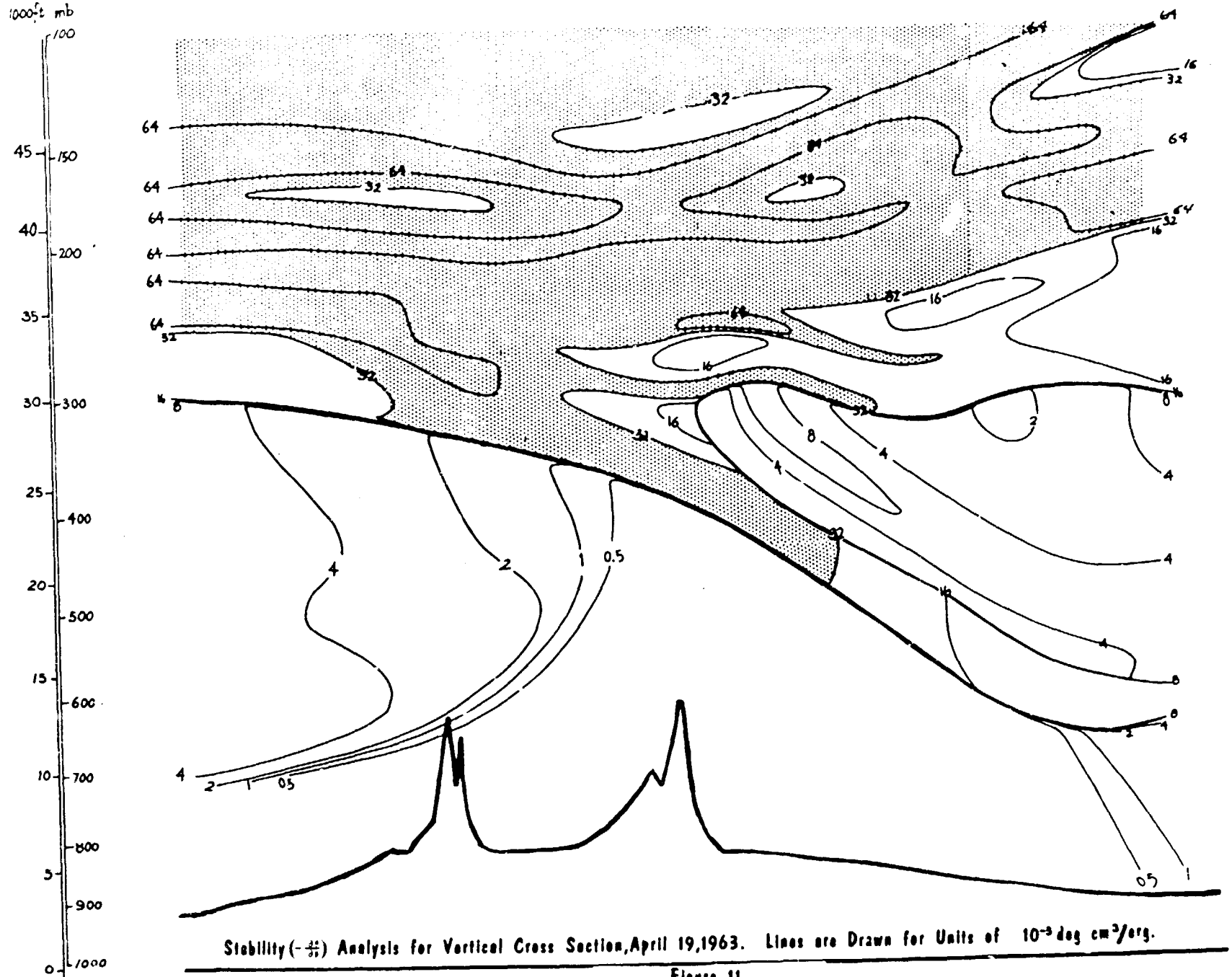

Stability ($-\frac{\partial\theta}{\partial z}$) Analysis for Vertical Cross Section, April 19, 1963. Lines are Drawn for Units of 10^{-3} deg cm^3/erg.

Figure 11

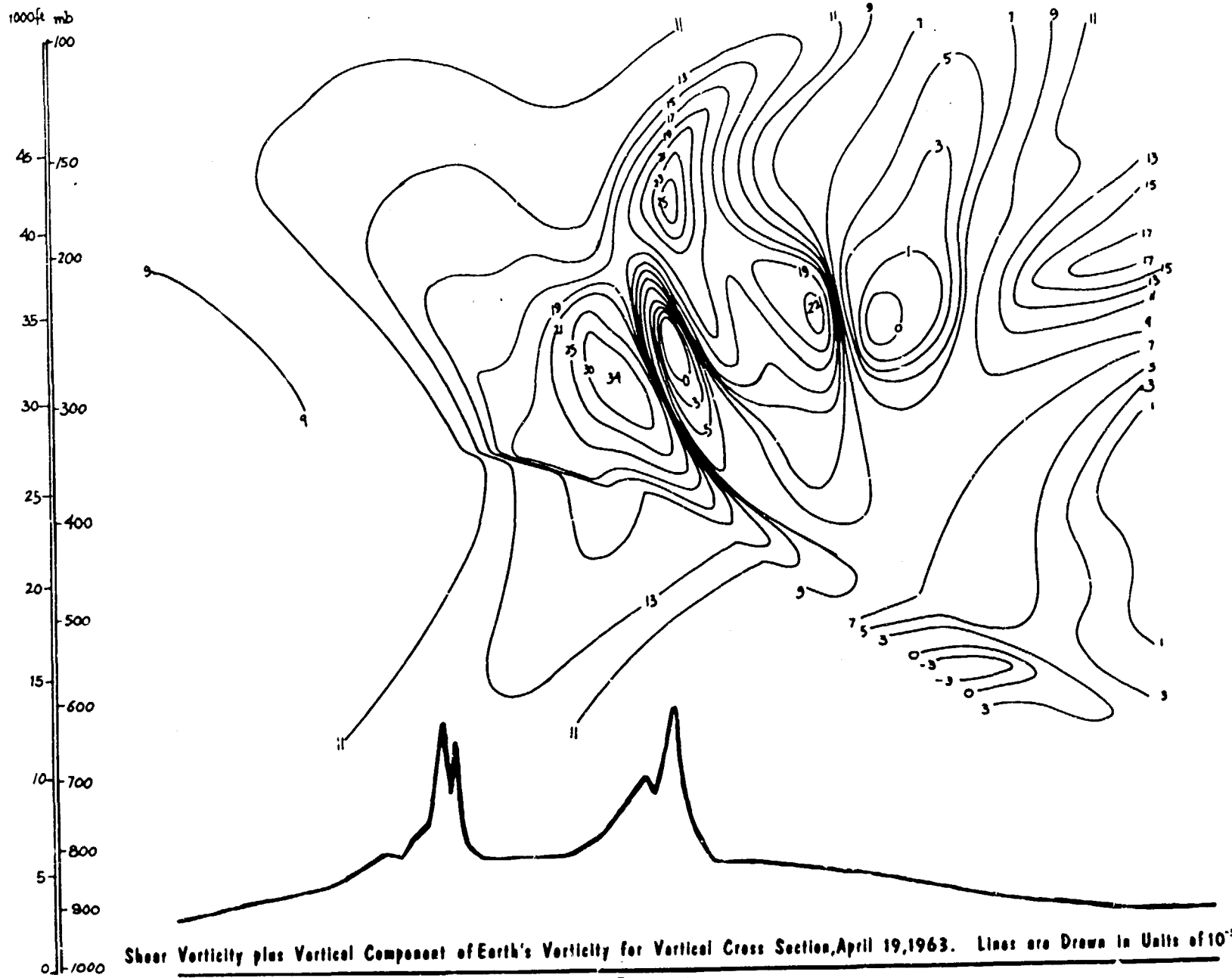

Shear Vorticity plus Vertical Component of Earth's Vorticity for Vertical Cross Section, April 19, 1963. Lines are Drawn in Units of 10^{-5} sec^{-1}.

Figure 12

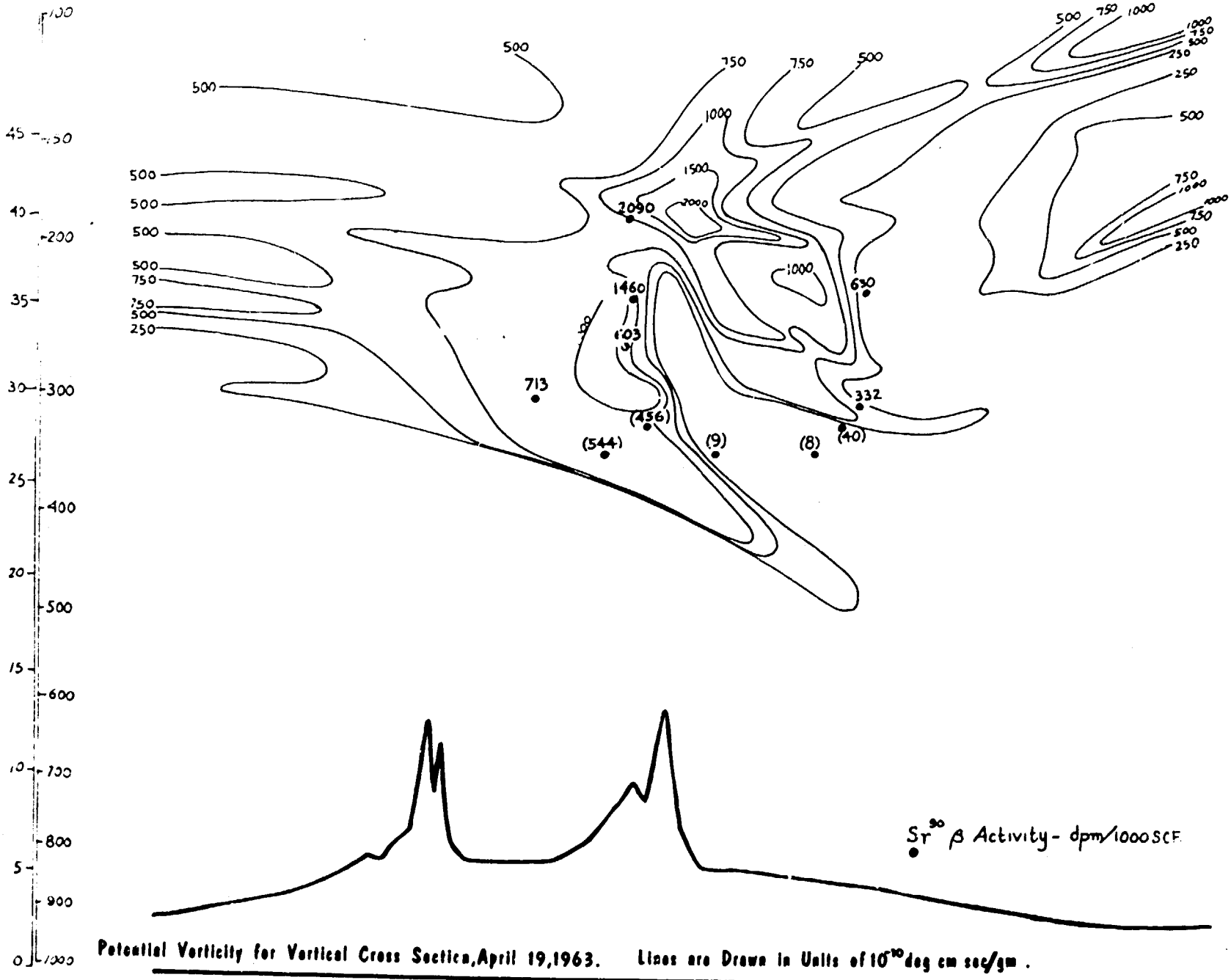

Potential Vorticity for Vertical Cross Section, April 19, 1963. Lines are Drawn in Units of 10^{-10} deg cm sec/gm .

Figure 13

The lines of constant stability in Figure 11 are drawn at an interval that progresses geometrically. The labeled range is from 0.5 to 64 x 10^{-5} $\frac{\text{deg-cm}^3}{\text{erg}}$, but values which approach zero are located inside the 0.5 line where the Θ lines are approximately vertical. This corresponds to the mixing layer generated by heating at the earth's surface. Values of stability greater than 32 x 10^{-5} $\frac{\text{deg-cm}^3}{\text{erg}}$ have been toned grey to facilitate recognition of the pattern. Note that the stability pattern is quasi-horizontally stratified.

By contrast the vorticity pattern is predominantly vertically oriented. The values range from 0 to 34 x 10^{-5} sec^{-1}, or about half the numerical range of the stability. The zeroes are located on the south or anticyclonic side of the jets in the stratosphere and upper troposphere. Negative values were calculated for the lower portion of the tropospheric frontal zone. These correspond to very strong anticyclonic shears which probably result from the vertical mixing of low momentum through the adiabatic layer into the frontal zone. The adiabatic layer extends down to the ground where the low momentum originated.

The product of the stability and the vorticity, shown in Figure 13, ranges from 0 to 2000 x 10^{-10} $\frac{\text{deg-cm-sec}}{\text{gm}}$. As one might anticipate, the potential vorticity pattern is complicated but two features

stand out clearly: (1) large values of P_Θ extend from the cyclonic stratosphere into the troposphere, and (2) small values of P_Θ extend from the troposphere into the anticyclonic stratosphere. These extensions are compatible with the folding process and the conservation of potential vorticity. The extension of tropospheric air into the anticyclonic stratosphere is consistent with the transformation from vorticity to stability, i.e., under divergence at constant Θ the vorticity decreases as the stability increases. Since the stratosphere is identified only on the basis of average stability, this mode of exchange must be recognized as possible.

If the pattern were produced by folding we should expect a positive correlation between the radioactivity and the values of P_Θ. The black dots in Figure 13 identify the locations of the WB-50 and RE-57 filter samples. Plotted adjacent to the dots are the β activities of Sr^{90} in disintegrations per minute per 1000 standard cubic feet of air.

The Sr^{90} activities are presented here because they serve as a standard for comparison with the activities of previous samples taken by the RB-57's and WU-2's. At the time of this writing, the chemical analysis of some of the samples has not been completed. The Sr^{90} activities for these samples were computed from the total β activities using an empirically derived relation,

$$Sr^{90} \text{ dpm/1000 SCF} = 4 \times \beta \text{ dpm/SCF}$$

In Figure 13 the computed activities are enclosed in parentheses.

We note that the Sr^{90} activities correspond rather closely to the values of P_Θ. The numerical similarity is accidental, but fortuitous for purposes of comparison. The range from 8 to 2100 dpm/1000 SCF approximates the P_Θ range from 0 to 2000 x 10^{-10} $\frac{\text{deg-cm-sec}}{\text{gm}}$ but the maxima do not coincide. The actual correspondence may be better or worse. Uncertainty in the positioning of the P_Θ lines derives primarily from the interpolations in the isotach field. If the RB-57's could have made wind measurements as did the WB-50's, this uncertainty would be greatly reduced.

The potential vorticity pattern does offer an explanation for the tropospheric sample, previously mentioned, which had a high β activity of 78 dpm/SCF. This sample was taken from the layer which extends from the cyclonic side of the central jet. The Sr^{90} activity was 332 dpm/1000 SCF, and the potential vorticity is greater than 250 and less than 500 x 10^{-10} $\frac{\text{deg-cm-sec}}{\text{gm}}$.

No samples were taken in the stratosphere where the P_Θ values are extremely low. We have no direct evidence that this is tropospheric air. However, this cross section brings to mind another, previously published report, Danielsen (6), in which a WU-2 took stratospheric

samples before and after crossing the jet. On the anticyclonic side, where P_θ was small, the Sr^{90} activity was 0.2 dpm/1000 SCF while on the cyclonic side it was 40 dpm/1000 SCF.

These samples were taken in the spring of 1960 when 0.2 and 40 dpm/1000 SCF were representative of tropospheric and stratospheric air, respectively. The air on the anticyclonic side of the jet also contained Sr^{89} from the French Sahara Test of February 13, 1960 which is known to have been deposited in a stable tropospheric layer on the anticyclonic side of the subtropical jet.

Thus, the evidence from the 1960 case supports the assumption that the low values of P_θ extending from the troposphere into the anticyclonic stratosphere had a tropospheric origin. In any future aircraft sampling program it would be advisable to obtain samples in this region to test the assumption.

Mission of April 21 - 22. On April 21, 1963 the planes were sent to northern Nevada to monitor another possible case of stratospheric extrusion. This mission, successfully completed by all aircraft, provided the evidence missed on the previous mission. The surface and 300 mb maps are shown in Figures 14a and b. The cross section, drawn this time on a more expanded scale, is presented in Figure 15. As before, the θ lines are black, but drawn for a $4^{\circ}K$ interval, the

isotachs are red and the flight paths are purple. The cloud formations recorded by the WB-50 weather observers have been rendered in a turquoise hatching and a dust cloud is depicted by brown dots.

The WB-50's traversed the layer at 19,000; 21,500; 24,000, and 26,000 feet. Rapid wind speed and temperature changes were recorded with each traverse. The net changes in wind speed and temperature were similar in magnitude to those observed on the 18th. On the return flight, both aircraft took samples which had β activities of approximately 2 dpm/SCF in the warm air south of the stable layer. Returning through the layer the upper aircraft sampled near the warm boundary. The sample had an activity of 87 dpm/SCF. Outside the layer, on the cold side near the top of a cloud, the activity of the next sample was 12 dpm/SCF. Ascending to 26,000, the upper aircraft again sampled in the layer and obtained a β activity of 92 dpm/SCF.

The two samples in the layer were near the boundaries, but both had high activities. Both activities were similar to that of the RB-57 sample taken at 28,000 feet in the stratosphere. It is quite probable that a sample taken in the interior of the layer would have had an activity closer to the 163 dpm/SCF of the 29,000 foot RB-57 sample. Evidence for this will be found in the continuous counting traces. In either case, we know that the layer contained stratospheric air down to the 24,000 foot level.

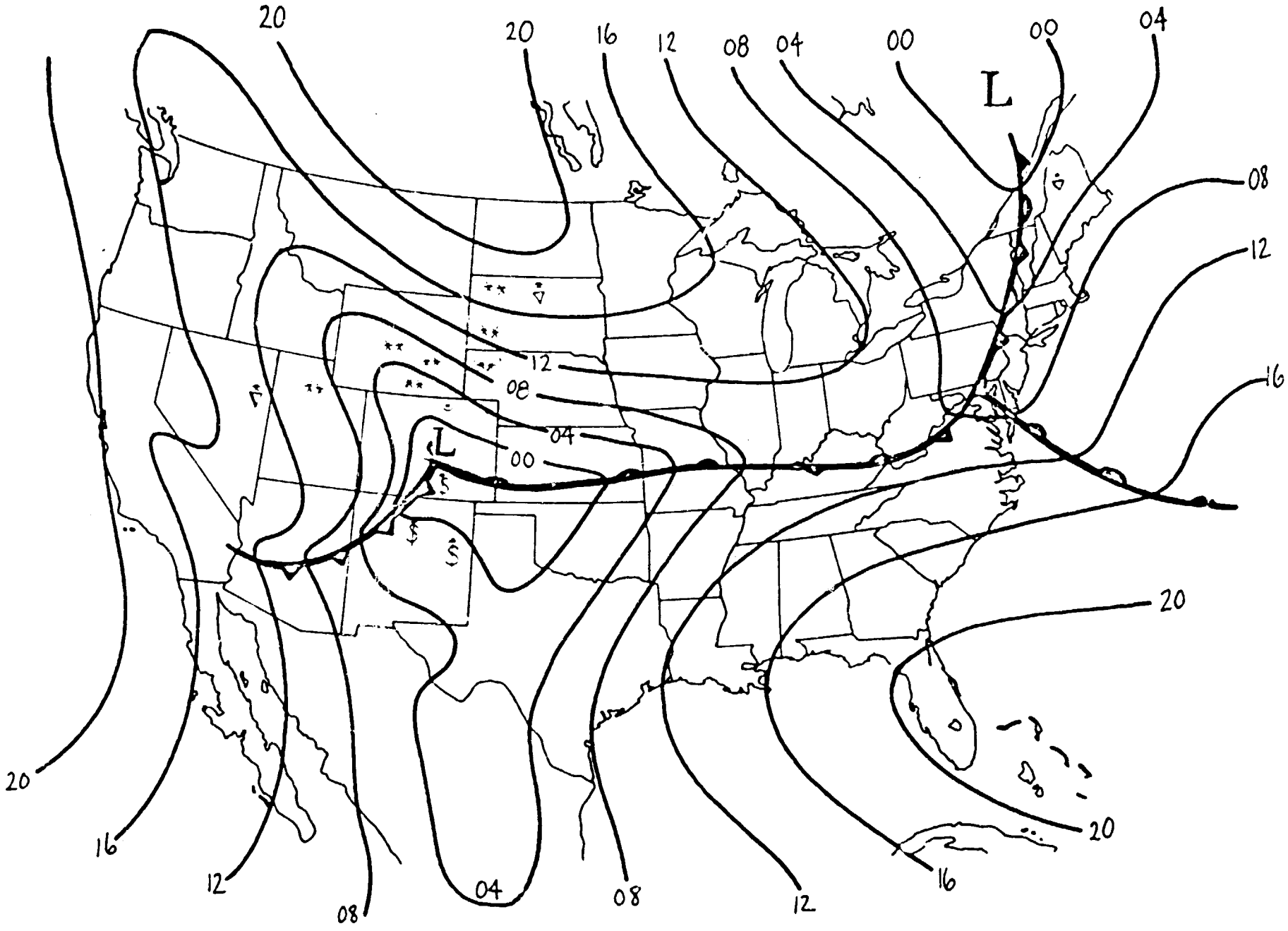

Figure 14a Surface Map-April 22,0000z,1963.

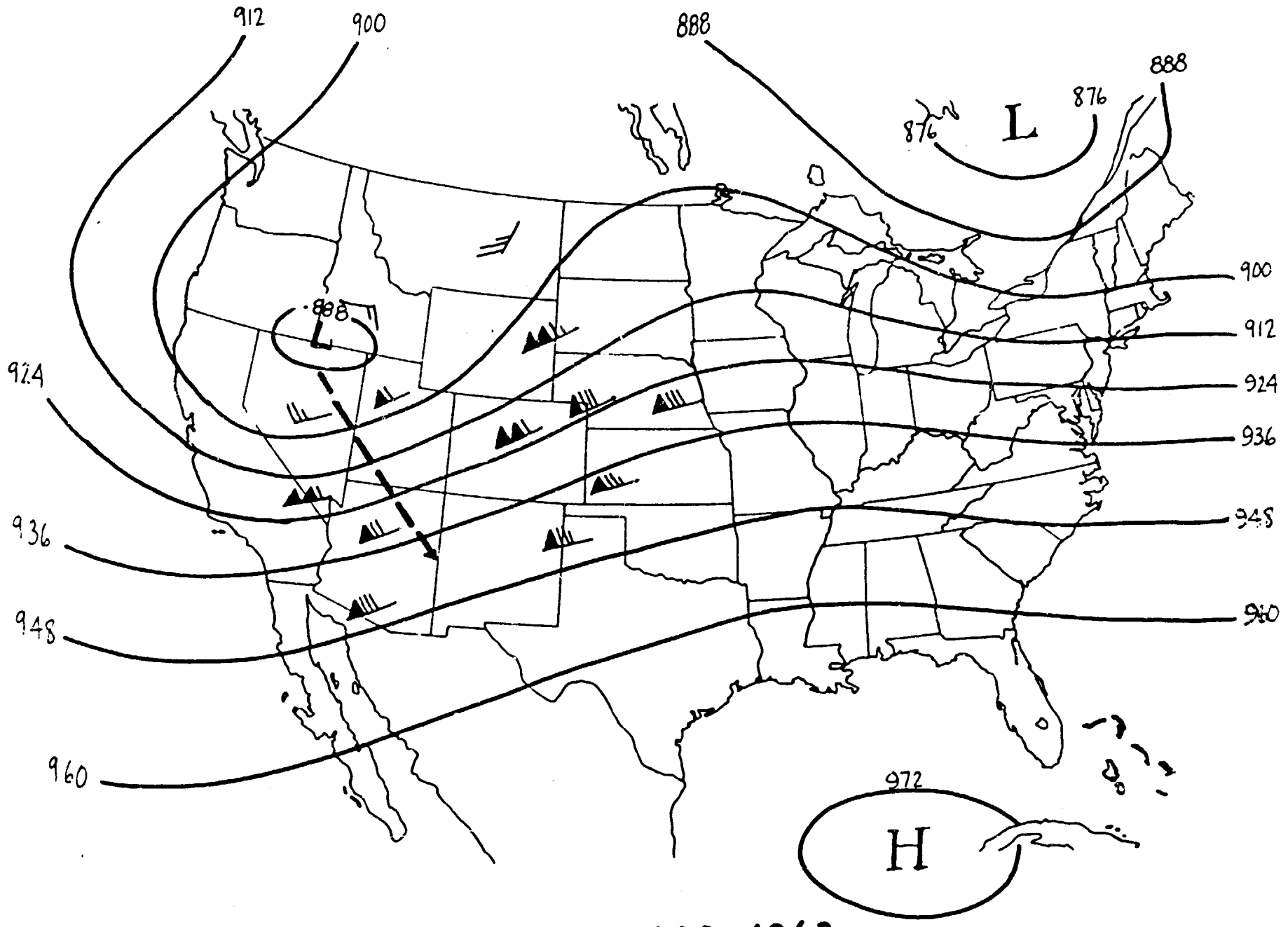

Figure 14b 300mb-April 22,0000z,1963

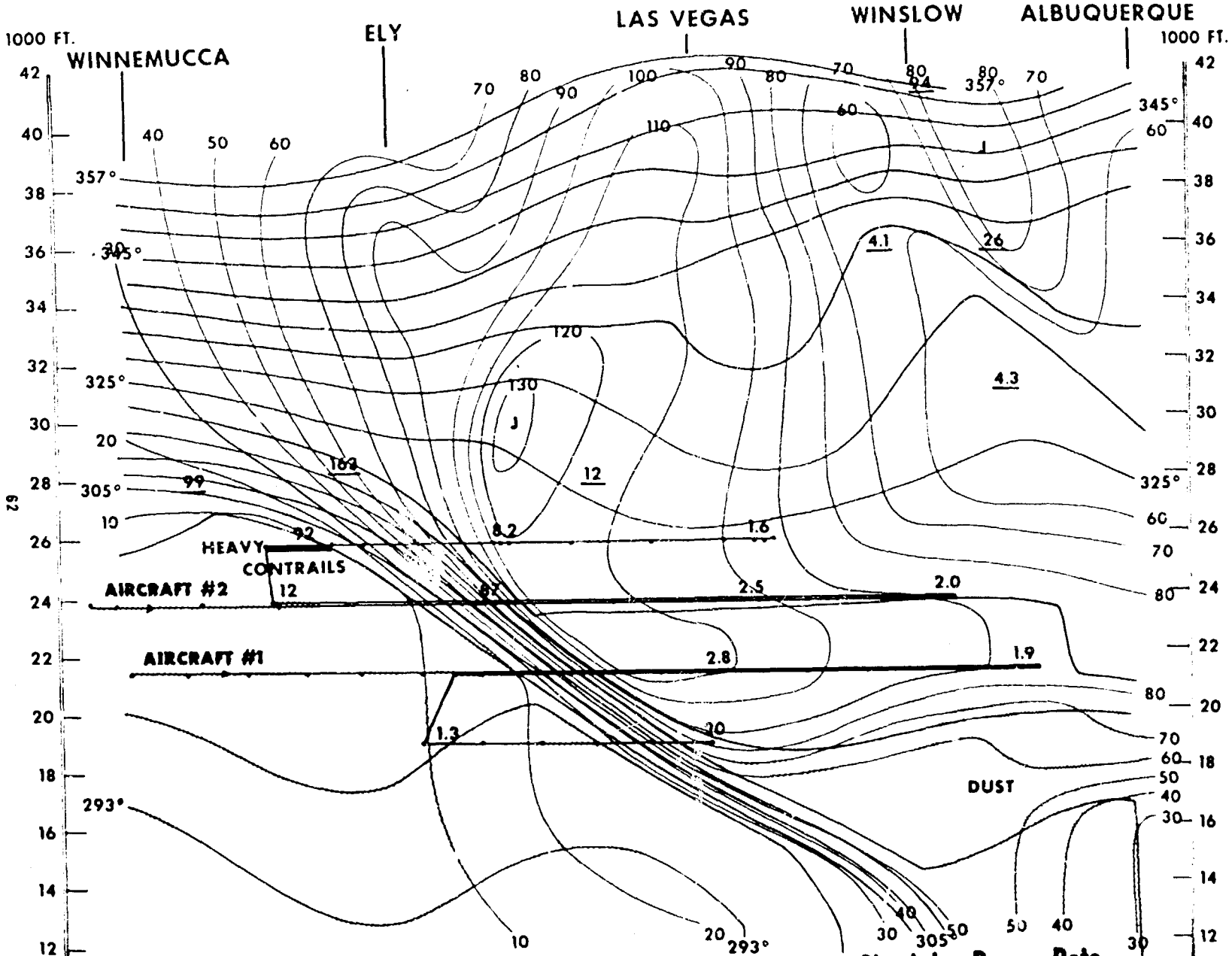

Figure 15 Vertical Cross Section for April 22, 1963, 0000z. Dust Cloud by Brown Dots. Clouds Indicated by Turquoise Hatching. Remaining Color Code same as Figure 9.

The lower aircraft did not take a sample in the layer at 21,500 feet, but did at the 19,000 foot level where the β activity was 20 dpm/SCF. Although down by a factor of four from that at 24,000 feet, this is still one order of magnitude greater than the tropospheric activities.

Although aircraft #1 did not take a sample in the layer at 21,500 feet, the continuously exposed filter paper was monitored during the entire flight. A portion of the counting rate trace is reproduced in the lower diagram of Figure 16 as a heavy continuous line. The thin line connects the observed temperatures. Directly above, with the same abscissa, are the counting rate and temperature traces recorded by aircraft #2 at 24,000 feet.

The traces for the two aircraft are remarkably similar. At both elevations the increase in temperature across the layer was 18°C and the increase in counting rate was 2,700 cpm. Outside the layer in the warmer tropospheric air the temperatures were approximately constant and the counting rate increased only slowly. On the return flight across the layer the traces of the two aircraft differed. This difference was produced by a change in flight path. Just after aircraft #2 re-entered the layer, the pilot turned 90° left to take a sample upwind. The original flight path was not quite orthogonal to the layer so after the 90° turn, the plane approached the warm boundary

Flight Data for WB50's, April 21-22, 1963

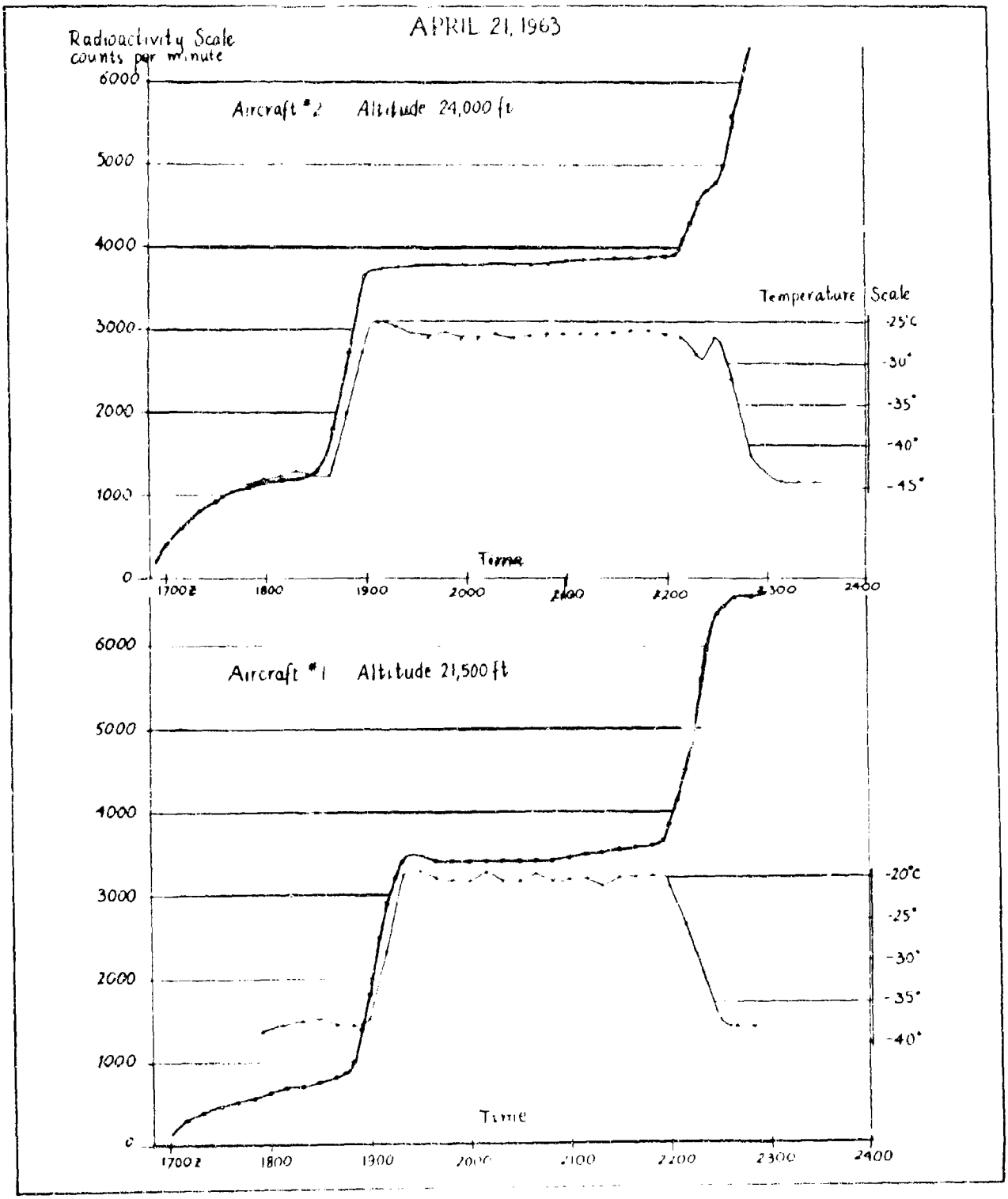

Figure 16

again. This accounts for the initial drop in temperature beginning at 2110 Z and the succeeding rise. When the sample was completed at 2130 Z and the pilot resumed his original heading, the temperature dropped rapidly again. Note that as the plane approached the warm boundary, the slope of the counting rate trace decreased. The sample, therefore, was not taken in the air with the richest concentration. The activity of the sample, 87 dpm/SCF, is proportional to the average slope of the trace over the 20 min interval. The average slope for the time of sampling was almost half the slope which characterized the layer. Therefore, as mentioned previously, an activity of 160 dpm/SCF would seem appropriate to the layer at 24,000 feet. A slightly lower activity, about 140 dpm/SCF, would be expected at 21,500 feet. Since the counting rates had the same slope, the ratio of activities should be inversely proportional to the ratio of the air densities, i.e., 1.15.

The continuous counting traces offer excellent proof that the stratospheric air extends to the 21,500 foot level with little dilution in its concentration of radioactivity. The trace recorded at 19,000 feet is not reproduced here, but as the airplane crossed the layer, the radioactivity trace showed two steps instead of one. Each step , although of short duration, had a steep slope. This indicates mixing by smaller scale folding between the tropospheric air in the frontal

zone and the extruded stratospheric air. The mixing appears to be along the Θ surfaces, not along the Θ gradient. In this way the radioactivity is diffused into the tropospheric frontal zone.

If the diffusion extended the radioactivity to the 12,000 foot level, it would have been rapidly mixed down to the ground. The concentrations would be diluted, of course, by mixing with the tropospheric air, but higher than normal surface concentrations would be expected. Figure 17 illustrates that the mixing below 12,000 feet was rapid. Below this level at Las Vegas, Winslow and Albuquerque the temperature lapse rates were adiabatic and superadiabatic.

At Albuquerque, which at the sounding time was just in advance of the front, the adiabatic layer extended up to 17,000 feet. On the basis of the moisture trace the upper limit of the mixing would appear to be 20,000 feet and this coincides with the top of the dust layer as reported by the WB-50 observers. Mixing through this unusually deep layer was promoted by the large scale downward transport of high momentum into the upper part of the mixing layer and strong heating from dry soil at the base of the layer. The high momentum, mixed downward, produced average surface winds exceeding 50 kts which in turn produced the dust storm. The pattern of the dust cloud shown in Figure 16 is in agreement with the WB-50 observations and the reports

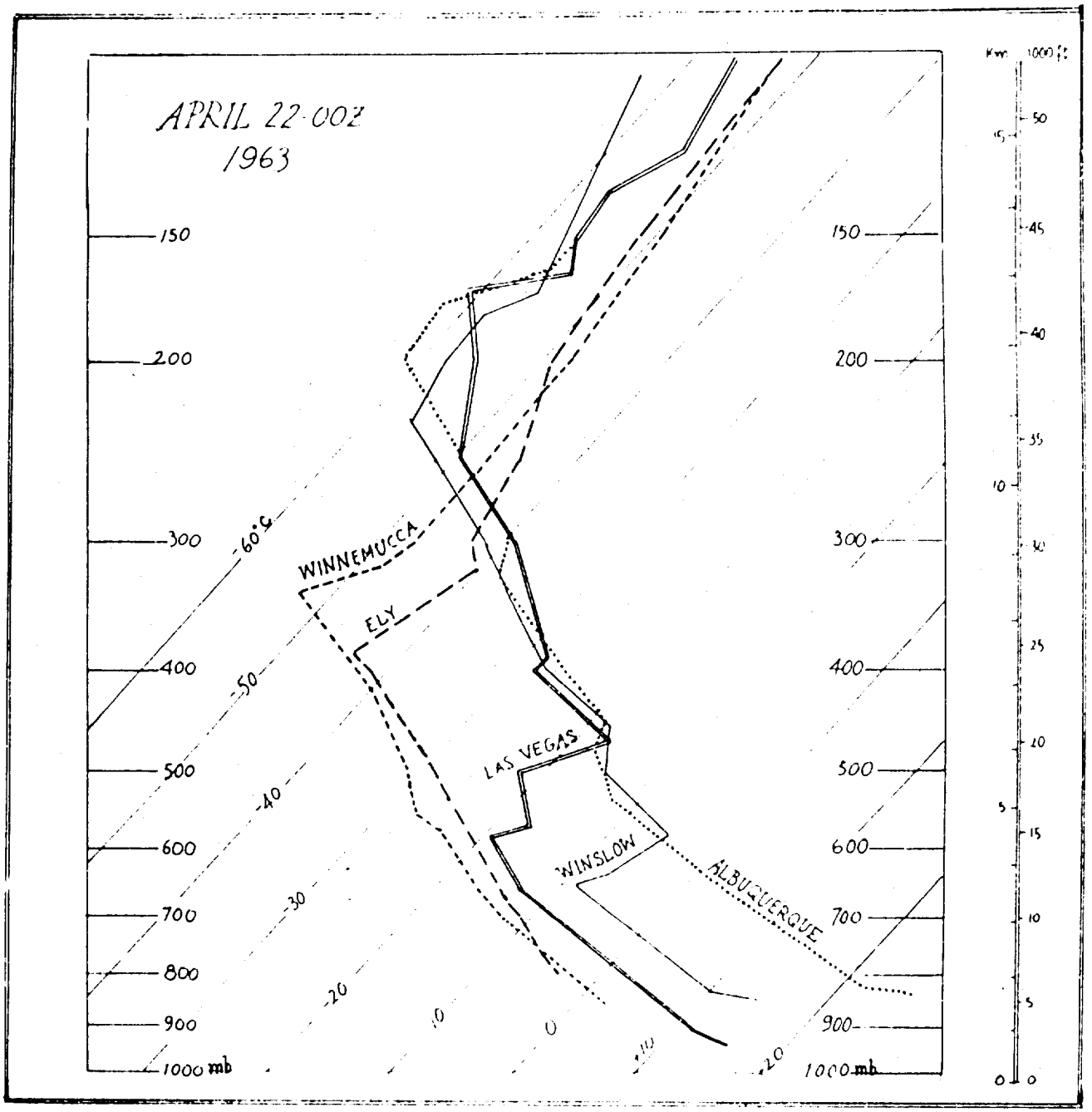

Temperature versus Pressure for Radiosonde Stations, April 22, Cross Section

Figure 17

of surface weather stations. Along and in advance of the front the dust obscured surface visibility, while just behind the front dust aloft was reported. It should be mentioned that Figure 16 extends to only 10,000 feet. Below this level, the front and the surfaces were vertical, i.e., the entire lower troposphere had an adiabatic lapse rate including the frontal zone.

From the aircraft measurements of radioactivity and the vertical mixing implied by the adiabatic lapse rates, dry fallout at the surface in the southern Rocky Mountain area should have been higher than normal. Measurements of the gross β activity of surface air made at four stations in this area by the Public Health Service are listed in the following table:

Field Estimates: Gross beta radioactivity of particulates in air.

	BETA ACTIVITY - dpm/SCF			
	April 20	April 21	April 22	April 23
Phoenix, Arizona	0.81	0.72	1.88	2.45
Las Vegas, Nevada	0.47	0.92	1.44	1.40
Santa Fe, New Mexico	0.82	0.59	1.24	----
Denver, Colorado	0.79	1.01	1.14	1.34

Values refer to samples collected during the 24 hour period ending in the morning of the date listed above.

The mixing which occurred on the afternoon of April 21 should have produced higher readings for the April 22 samples. All stations

showed an increase in activity on the 22nd and these activities were the highest in the United States for that day. The activities were not extremely high because the mixing extended through such a deep layer. Also, the values in the table represent a 24 hour integration, whereas the mixing was most active during the afternoon.

Assuming a background of 0.5 dpm/SCF for the tropospheric air and six hours of active mixing the activity of the mixture would have been roughly ten times that of the tropospheric air or 5 dpm/SCF. This, in turn, represents a mixture of about ten parts tropospheric to one part stratospheric air. Therefore, the stratospheric activity would have been about 50 dpm/SCF. This value checks out well with the activities deduced from the slopes of the continuous trace and the β activity of the sample at 19,000 feet. On the basis of the slope of the trace during the period of sampling the activity in the stratospheric air would be between 44 and 60 dpm/SCF at 19,000 feet. A more complete explanation of the traces will follow in the discussion of the potential vorticity.

To complete the discussion of the April 21 - 22 data we now turn to Figure 18 which contains the distribution of potential vorticity and the β activity of Sr^{90} captured in the airplane filter samples. The Figure corresponds to Figure 13 but the P_Θ values are drawn for a

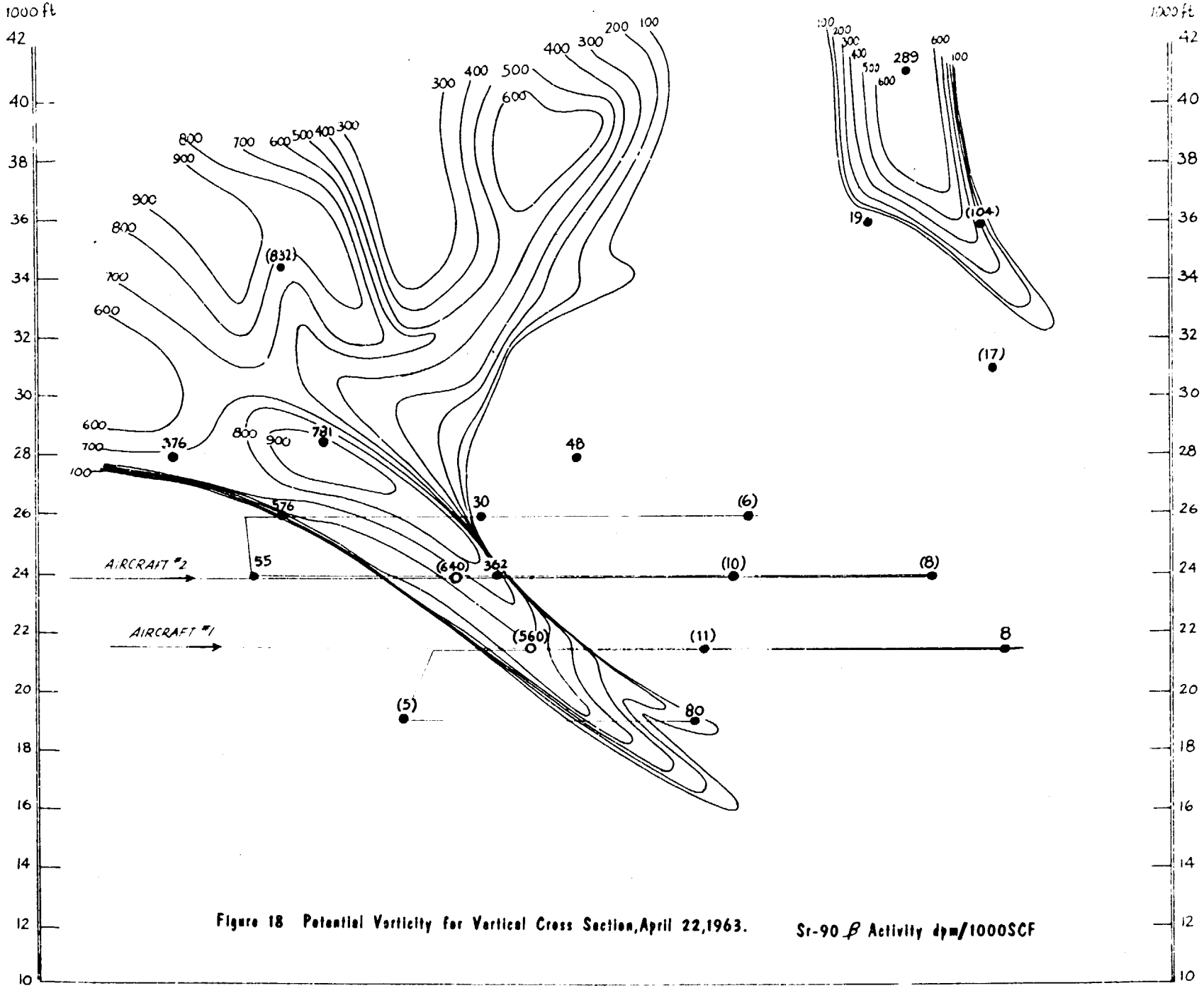

Figure 18 Potential Vorticity for Vertical Cross Section, April 22, 1963. Sr-90 β Activity dpm/1000SCF

constant interval of $100 \times 10^{-10} \frac{\text{deg-cm-sec}}{\text{gm}}$. As before, the Sr^{90} activities are plotted above a black dot which locates the position of each sample. Chemical analyses of some of the samples are still in progress, so once again parentheses denote the values computed from the total β activity. The two values plotted above white dots were computed from the continuous counting rate traces.

If allowances are made for the differences in the geometric scales of Figures 18 and 13, one notices that the P_Θ patterns are quite similar. Large values of P_Θ again extend from the cyclonic stratosphere into the troposphere and low values of P_Θ extend from the troposphere into the anticyclonic stratosphere. We notice also that the numerical correspondence between the P_Θ values and the Sr^{90} activities is again close. Almost all of the activities have a numerical value equal to the P_Θ value. The exceptions are at the left of the diagram where the 376 dpm/SCF appears to be too low for the stratosphere and 55 dpm/SCF is abnormally high for the troposphere. The latter was taken in a thin cirrus cloud near the top of a cumulonimbus. Its high β activity implies that the cumulonimbus penetrated and mixed with the stratospheric air at some earlier time. Further support for this can be drawn from the observations of contrails reported by the #2 WB-50. After completing the sampling at 24,000 feet, the pilot

took the plane up to 26,000 feet to retraverse the layer. At this point, instead of turning up wind to take another sample, the pilot exposed the filter while heading outbound from the I. P. on the main flight track. After a 10 min. exposure he reversed his heading and completed another 10 min. of exposure. The reversals in flight can be seen in Figure 15. During this operation heavy contrails were observed which became thin as the plane proceeded outbound from the I. P. and became heavy again on the return flight inbound. From the analysis of the cross section, and the observed wind, temperature and dew point changes it is clear that on the outbound from the I. P. the plane entered the stratosphere, then on the return flight it left the stratosphere and entered the troposphere again. The facts that the dew point dropped but was still measurable and the contrails thinned but did not vanish indicate the lower stratospheric air had been mixed with moisture-laden tropospheric air. The continuous radioactivity trace and the 92 dpm/1000 SCF on the sample confirm the presence of the stratospheric air.

As shown in Figure 18, the Sr^{90} activity for this sample was 576 dpm/SCF. This greatly exceeds the 368 which would be expected from the total activity. It also exceeds the value to be expected from the Cs^{137} activity. Reprocessing of the sample is in progress to determine whether an error was made in the Sr^{90} analysis. A value of 368 dpm/

1000 SCF would bring it in line with the 362 dpm/1000 SCF measured by the RB-57 and would support the conclusion that the lower stratospheric air had decreased its radioactivity and increased its moisture by cumulus cloud penetration and mixing. One may recall that on the April 18-19 mission the plane had entered the stratospheric layer and then had to ascend to stay on top of a cumulonimbus which had penetrated the layer.

A final comment: note that the tongue of large P_Θ extending from the stratosphere splits into two near the 19,000 foot level. It was mentioned earlier that the continuous radioactivity trace showed two steps rather than one. On the basis of the P_Θ values, the first step encountered should have had the steeper slope. The radioactivity trace confirms this. Also, the slope of both steps should have been less than the slope at 21,500 feet. Again the continuous trace supports this. If for purposes of comparison we set the average slope during the time of sampling at 19,000 feet as one, then the slopes increase as

1/2.2/3/5.5

for the second step, the first step and the step at 21,500 feet. Since the Sr^{90} of the sample at 19,000 feet was 80 dpm/SCF the Sr^{90} activity at 21,500 feet should be about 530 dpm/SCF if allowances are made for the air density variation. A value of 530 dpm/SCF compares favorably

with the value of 560 dpm/SCF previously estimated from the slopes and samples taken by the other aircraft.

Mission of April 22 - 23. The April 22-23 mission proved to be extremely interesting. The surface and 300 mb charts for April 23, 1963 at 0000 Z are shown in Figures 19a and 19b, respectively. Two WB-50's were sent to Salt Lake City. They were assigned a southeast flight track at 24,000 and 27,000 feet. Their meteorological and radioactivity measurements were at first difficult to understand. Fortunately, extra radiosonde ascents had been made at 1800 Z at all of the stations in the Rocky Mountain Basin. By constructing cross sections for 1800 Z on April 22 and 0000 Z on April 23 it was possible to interpret the observations.

The meteorological conditions over Utah were changing rapidly as the trailing edge of the dry extruded stratospheric layer was moving eastward and being replaced by moist tropospheric air. A well-defined layer of dry, stable air was present over Salt Lake City at 1800 Z but this layer was not evident on the sounding six hours later. When the WB-50 meteorological observations were begun at 1830 Z, both aircraft were southeast of the layer in the tropospheric air. Proceeding southeastward, the flight observer aboard the lower aircraft, #1, recognized that the layer to be monitored was farther to the northwest and he reversed his flight direction to encounter it. After passing through the

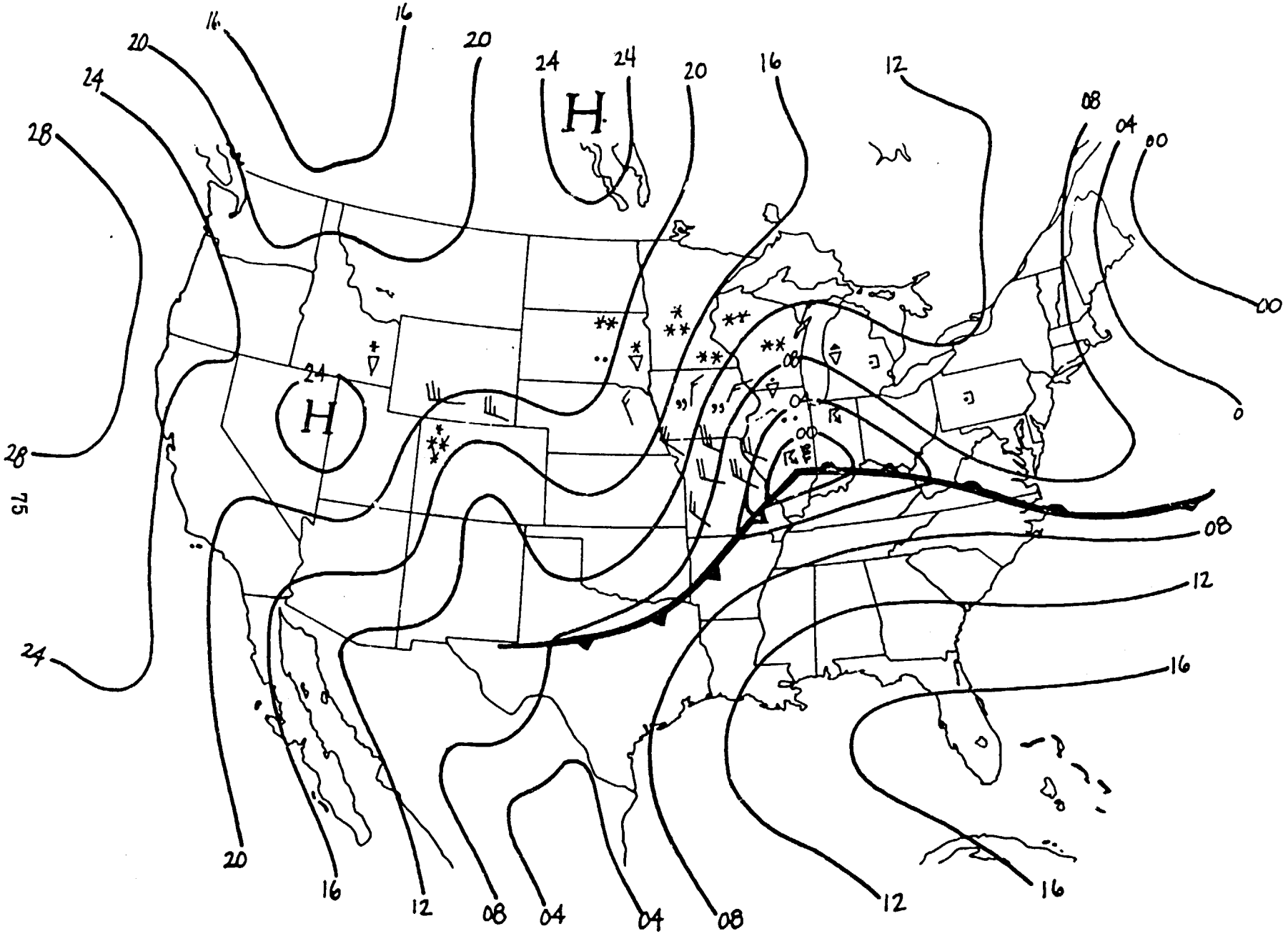

Figure 19a Surface Map-April 23,0000z,1963

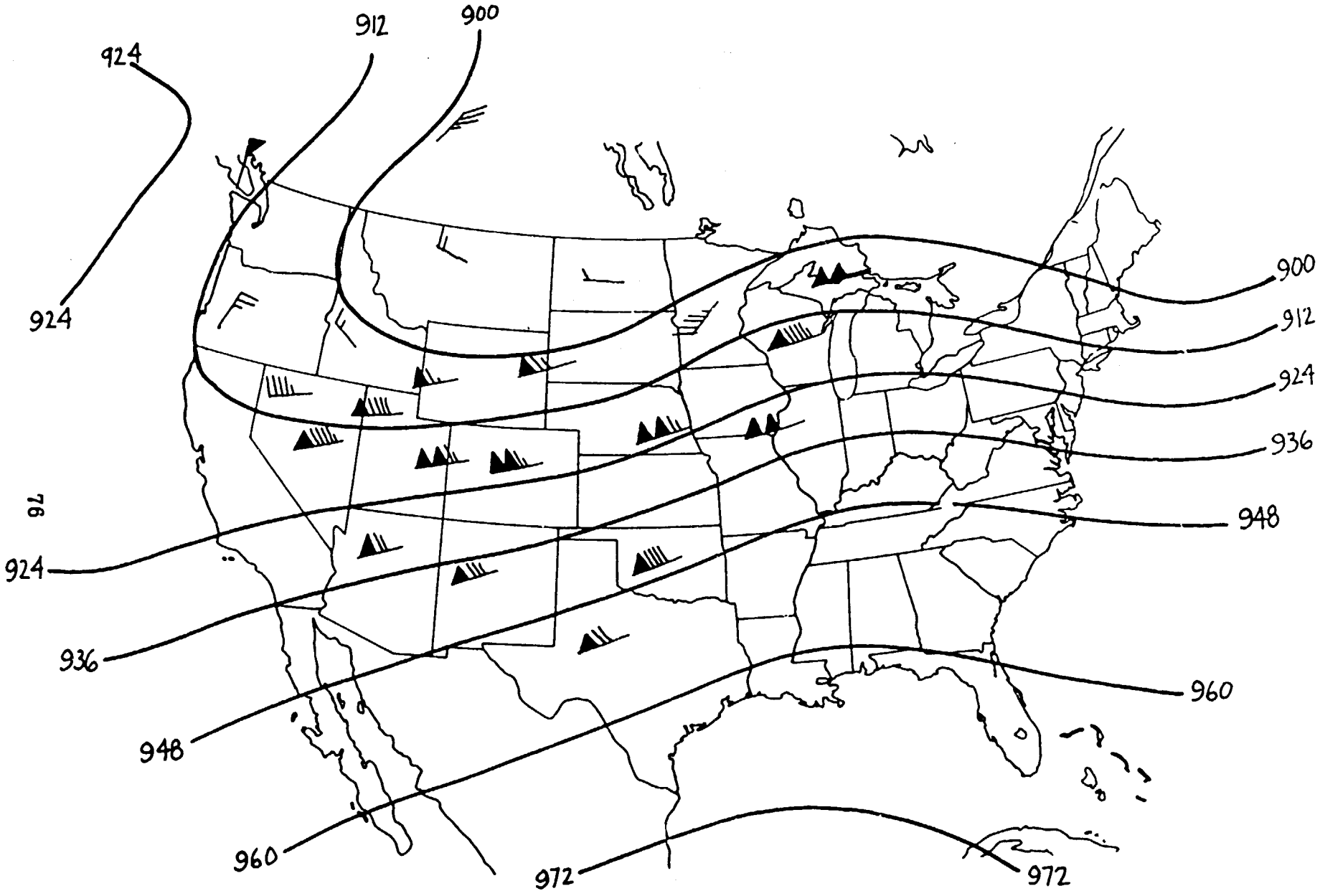

Figure 19b 300mb-April 23,0000z,1963

layer at Salt Lake City the original flight heading was resumed. The reversal in flight path is shown in Figure 20 but it should be kept in mind that this cross section was drawn from the 0000 Z radiosonde ascents, not the 1800 Z ascents. As is also evident in Figure 20, the upper aircraft, #2, proceeded southeastward almost to Albuquerque before reversing its heading.

Between Salt Lake City and Grand Junction aircraft #2 passed through a narrow stable layer denoted by the three closely spaced Θ lines in Figure 20. The temperature trace in the upper diagram of Figure 21 shows a rapid rise of $4^{\circ}K$ as the plane crossed the layer at about 1900 Z. Notice that the radioactivity trace maintained a small slope characteristic of tropospheric air during transit of the layer. The same layer was crossed by aircraft #1 at 2050 Z, lower diagram in Figure 21, and again the radioactivity trace remained unchanged.

Similar traces were reproduced on the return flights. Aircraft #2 recrossed it at 2200 Z, aircraft #1 at 2120 Z. Obviously this layer was generated entirely from tropospheric air. The potential vorticity would also indicate that the layer was formed from tropospheric air by frontogenesis because $\mathcal{L}_p > 0$ and $\mathcal{L}_\Theta < 0$.

After aircraft #2 returned to Salt Lake City it ascended from 27,000 to 29,000 feet. During the ascent, which began at 2200 Z,

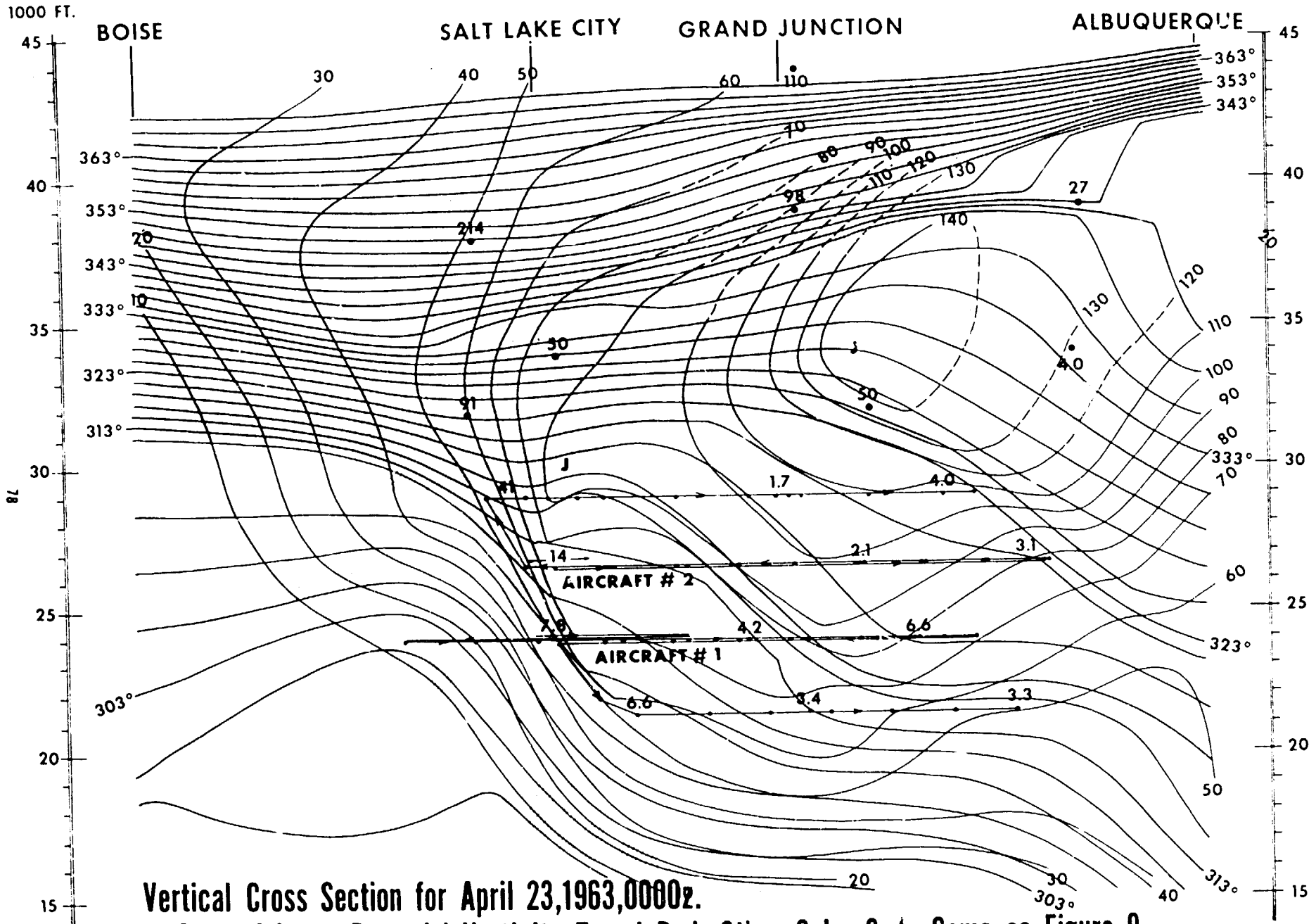

Vertical Cross Section for April 23,1963,0000Z.
Area of Large Potential Vorticity Toned Red, Other Color Code Same as Figure 9.

Figure 20

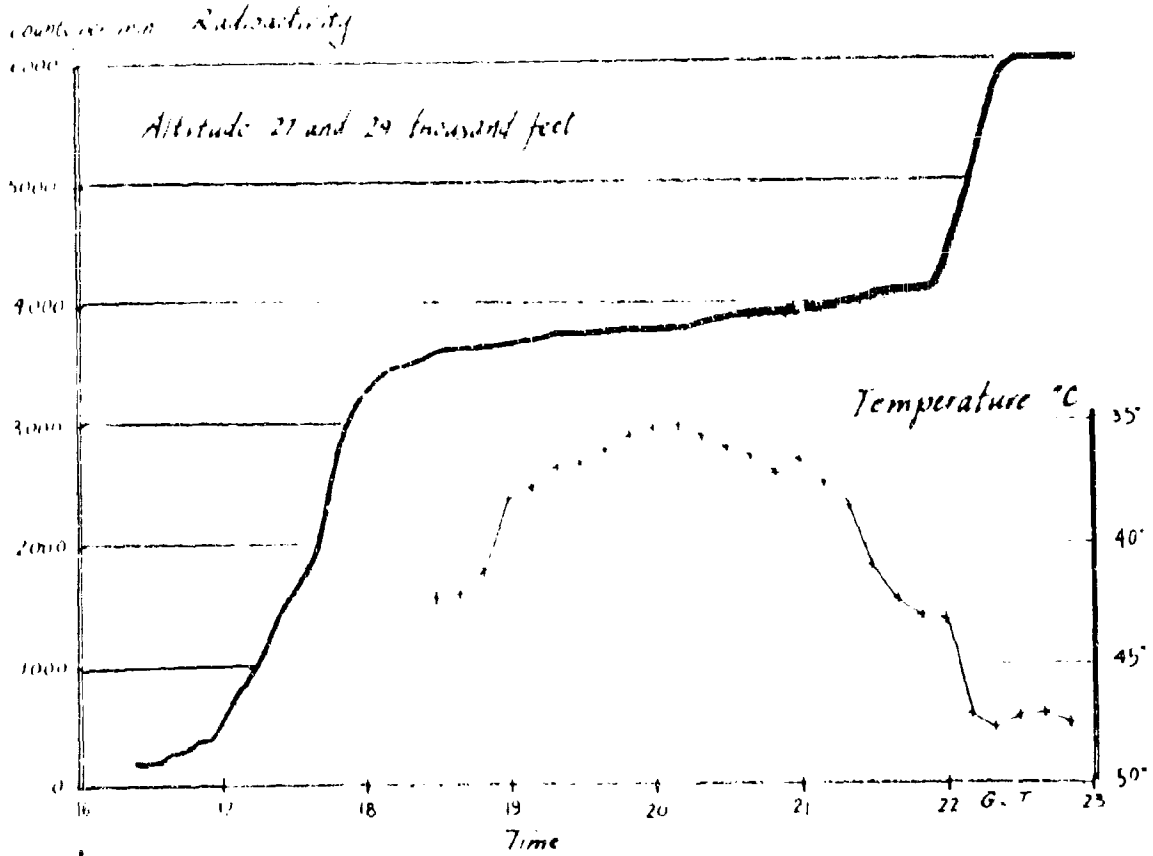

Flight Data 22 April 1963
Altitude 24 thousand feet.

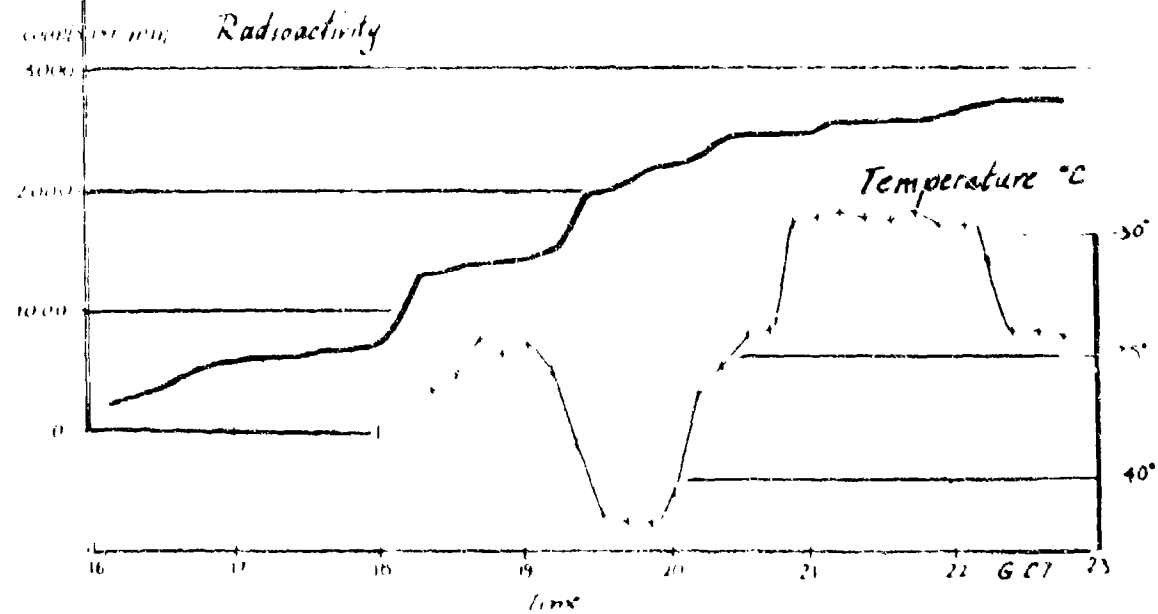

Figure 21 Flight Data for WB50's

the temperature decreased rapidly and the radioactivity accumulation increased rapidly. The stability was too low to be considered stratospheric, but the wind shear was strongly positive both at constant p and constant Θ. Figure 22 shows the Salt Lake City sounding for 0000 Z. The letter T and the arrow locate the coded tropopause at approximately 32,000 feet.

This is an excellent example of the difficulty in classification and interpretation which follows from the conventional definition of the tropopause. Stratospheric air with large values of potential vorticity may be destabilized by convergence at constant Θ until it no longer meets the criteria. During the destabilization the vorticity has increased but this does not enter into the usual definition. In this case, the vorticity is extremely large in the air beneath the coded tropopause. The radioactivity proves it is stratospheric air.

To assist the viewer, Figure 20 has been toned red where the values of P_Θ are representative of stratospheric air. This pattern should be compared to the pattern which would be obtained if one drew a smooth tropopause curve through the little red T's in Figure 20 which represent the coded tropopause at the sounding stations. As in the previous two cases, we find the radioactivity samples in agreement with the potential vorticity distribution but not in agreement with the conventional stratosphere.

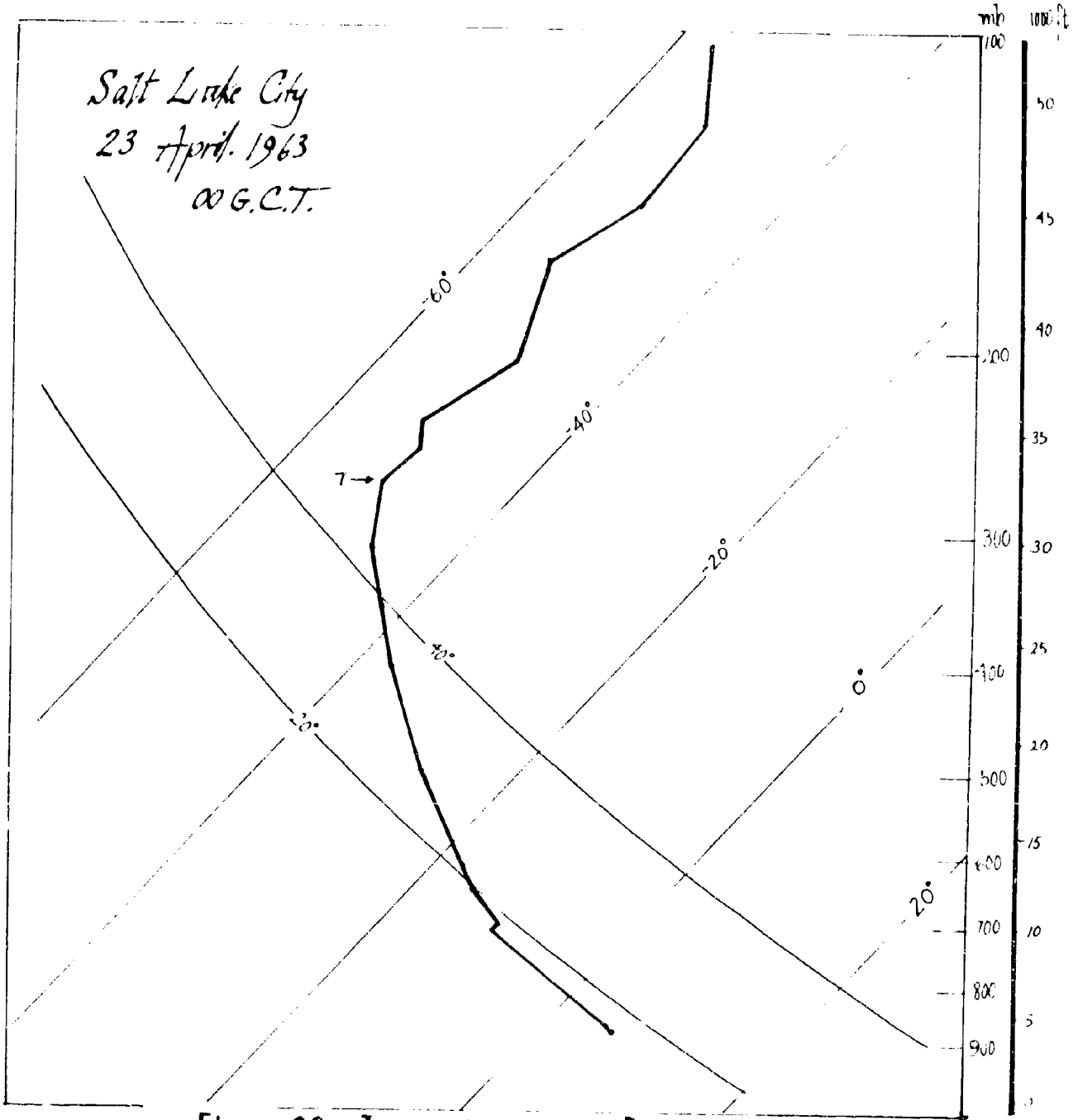

Figure 22 Temperature versus Pressure

It should also be noted that aircraft #2 accumulated considerable radioactivity, 3,200 cpm, while enroute to the I. P. at Salt Lake City. Unfortunately, meteorological observations were not made while the planes were enroute to the I. P. and the flight plans were not saved. But after recent discussions with crew members of the WB-50's, it appears that this accumulation occurred during a gradual ascent to the flight altitude after crossing the Sierra Nevada Mountain range. The cross section for 1800 Z, valid during the ascent, shows the extruded stratospheric layer sloping down from Salt Lake toward the Sierras. One reasonable interpretation is that the plane ascended at a slightly greater slope than that of the layer. Therefore, it passed from beneath the layer to above the layer just before reaching Salt Lake. Turning southeast along the flight track, aircraft #2 then remained above and south of the layer.

Aircraft #1 ascended through the layer at Salt Lake, proceeded southeast and then reversed its flight heading as previously mentioned. The radioactivity and temperature traces, lower diagram Figure 21, show an increase in slope of the accumulated radioactivity at 1800 Z then a decrease in slope at 1820 Z. These changes must have been due to an ascent through the layer. On the return northwest flight, the radioactivity took another short duration step at 1910 Z. After it leveled

off again the temperature continued to drop. Only a narrow zone contained the stratospheric air as indicated by the red shading in Figure 20 at 24,000 feet. On the third pass across the layer, the net rise in radioactivity was about the same as on the two previous passes, but it was less well defined in time and space.

Isentropic Trajectories, April 21 - 23. While the flights were in progress over Utah, tornadoes were forming in east central Illinois. As shown on the surface map, Figure 19, they formed near the center of the low. Mr. Glenn Stout, operating the radar for Project SPRINGFIELD, kept them under surveillance as they passed eastward across the southern portion of the Illinois Water Survey Network. Since tornadoes frequently form along the leading edge of the extruded stratospheric air, the author wanted to determine whether the stratospheric air could be traced to this tornado region.

Trajectories were computed on the 295, 300 and 305^{O}K isentropic surfaces by calculating backwards in time from Dayton, Ohio; Peoria, Illinois; Columbia, Missouri; and the approximate location of the tornadoes. The trajectories are presented in color in Figure 23. The color code is given in the upper right of the diagram. For this report we are most interested in the red and purple trajectories which originated in northern Idaho and southern Oregon at 1200 Z, April 21. These

Figure 23

ISENTROPIC TRAJECTORIES TERMINATING APRIL 23, 1963-00 G.C.T.

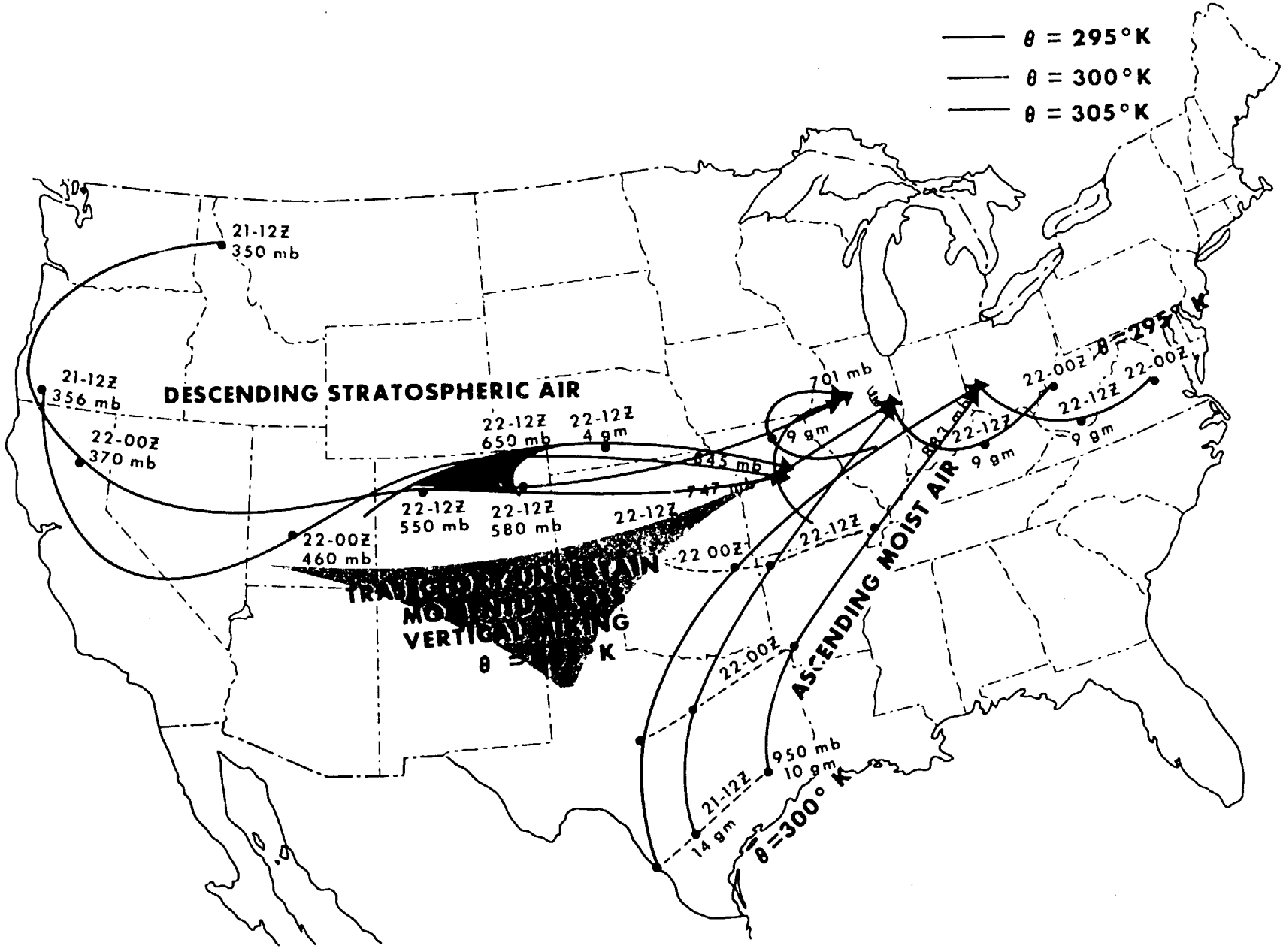

trajectories started in the stratosphere at about 350 mbs. The air descended as it moved around the upper level cyclone. When it moved across Nevada the 300°K air was near the base of the extruded layer which was sampled by the WB-50 #2 aircraft, (see Figure 15), and the 305°K air was in the lower stratosphere which was sampled by the RB-57 aircraft. We know, therefore, that this air was stratospheric.

As the air moved eastward during the 22nd it turned anticyclonically and continued to descend to 500, 600, and 700 mbs as it approached Peoria and Columbia. On the 305°K isentropic chart for 0000 Z, April 23, this stratospheric air appears as a jet of dry air moving at 50 - 75 knots across southern Nebraska, northern Missouri and central Illinois. The eastern limit of the stratospheric air cannot be precisely determined, but the evidence indicates that it extended up to the tornado region. East of this point the trajectories originated in the south, near the Gulf of Mexico, and in the southwest. The trajectory method could not be applied to the southwest flow because the momentum was modified primarily by vertical mixing in an adiabatic layer.

It is clear from Figure 23 that the tornadoes were forming in a region of strong confluence -- vertical as well as horizontal. Stratospheric air, confirmed by the aircraft samples, was descending into the development region and may have played an important role in the tornado

formation. It must be remembered that the stratospheric air had a large value of potential vorticity. Under the action of a concentrated field of convergence this air could develop an intense cyclonic spin before it would become turbulent. In laboratory models of intense vortices the introduction of turbulence into the fluid destroys the vortex. The author and Mr. Larry Davis are of the opinion that the intense spin develops in the stratospheric air which descends in the core of the tornado. This descending air would not produce a radar echo unless copious amounts of water or hail were falling into it. The echo free volume which appears on many of the radar photographs of tornado clouds may be explained by this phenomenon. At the present this is purely a hypothesis. Several tornado cases are currently being investigated to see if air with large values of potential vorticity entered the region of tornado development.

Mission of May 3 - 4. The missions previously discussed were selected to test the theory of tropopause folding. A stable layer thought to be of stratospheric origin was monitored in each case. Positive results were obtained. The mission of May 3 - 4 was designed to test the opposite case. At a time when no extruded layers were expected, the WB-50's were sent to monitor the radioactivity to see if the activities were consistently low.

On May 3, two WB-50's were sent from Scott AFB, Illinois to McClellan AFB, Sacramento, California. Aircraft #1 flew at 20,000 feet while aircraft #2 flew directly above it at 26,000 feet. Filters were changed every 20 minutes so that no gaps would exist in the data. Also, both aircraft monitored a continuously exposed filter paper.

The synoptic charts are shown in Figure 24. Notice the rain showers reported over the Rocky Mountains. The planes flew at latitude 40°N but diverted course slightly to avoid sampling in the water clouds. Water clouds damage the filter paper and upset the flow rate through the filter.

Figure 25 shows the flight cross section drawn from the May 4, 0000 Z radiosonde data and the aircraft measurements. The Θ lines are drawn from every 2°K and the clouds are depicted by hatching. Dashed lines depict the flight paths which contain the total β activities in dpm/SCF. At 26,000 feet the activities ranged from 0.8 to 6 dpm/SCF and averaged 2.96 dpm/SCF. At 20,000 feet the activities varied from 0.5 to 2.2 dpm/SCF and averaged 1.65 dpm/SCF. All of these values were characteristic of the tropospheric air sampled on the previous missions. No large values were encountered.

Samples taken by the RB-57 aircraft are also plotted on Figure 25 at North Platte and between Salt Lake City and Winnemucca. The

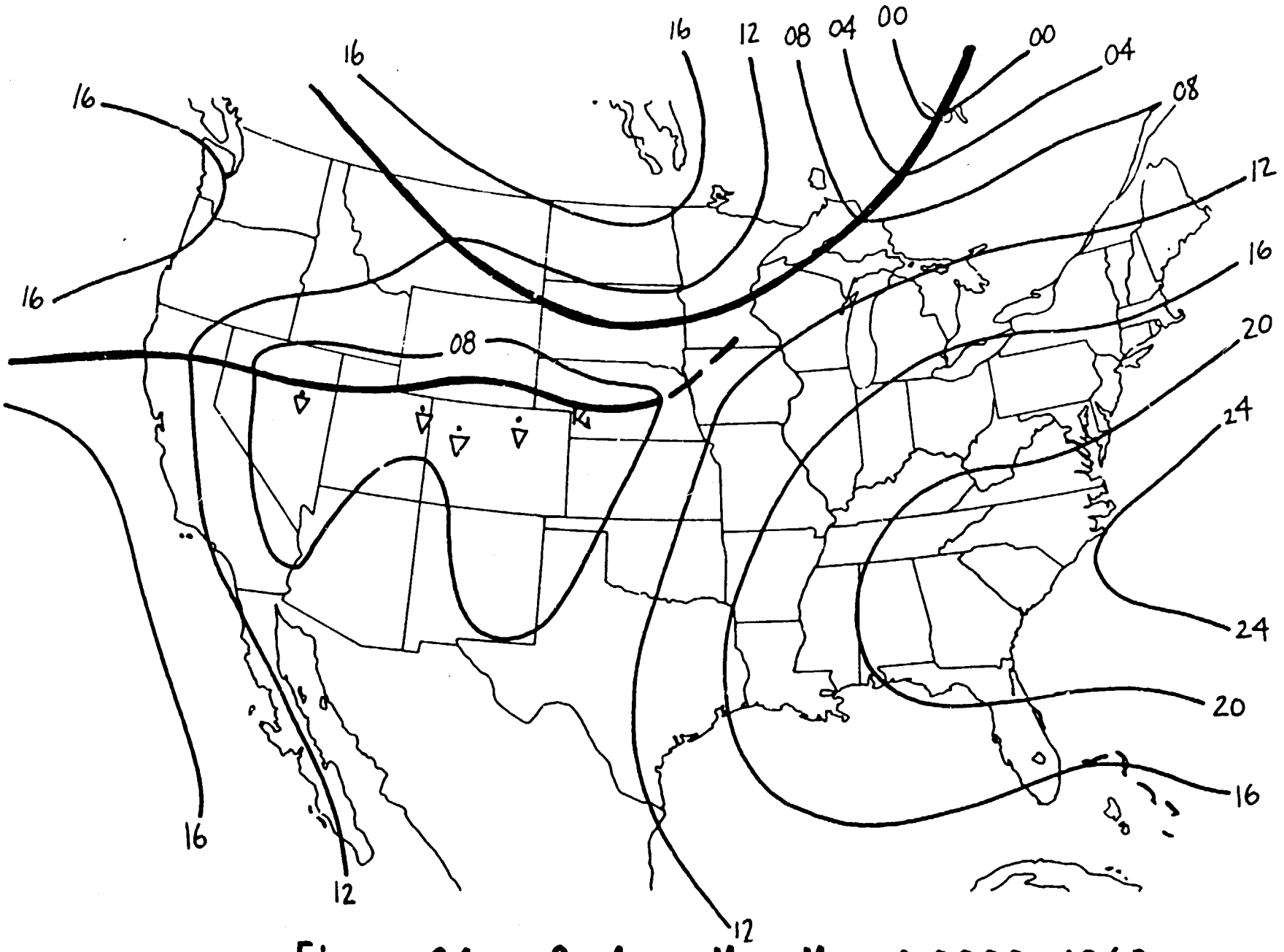

Figure 24a Surface Map-May 4,0000z,1963

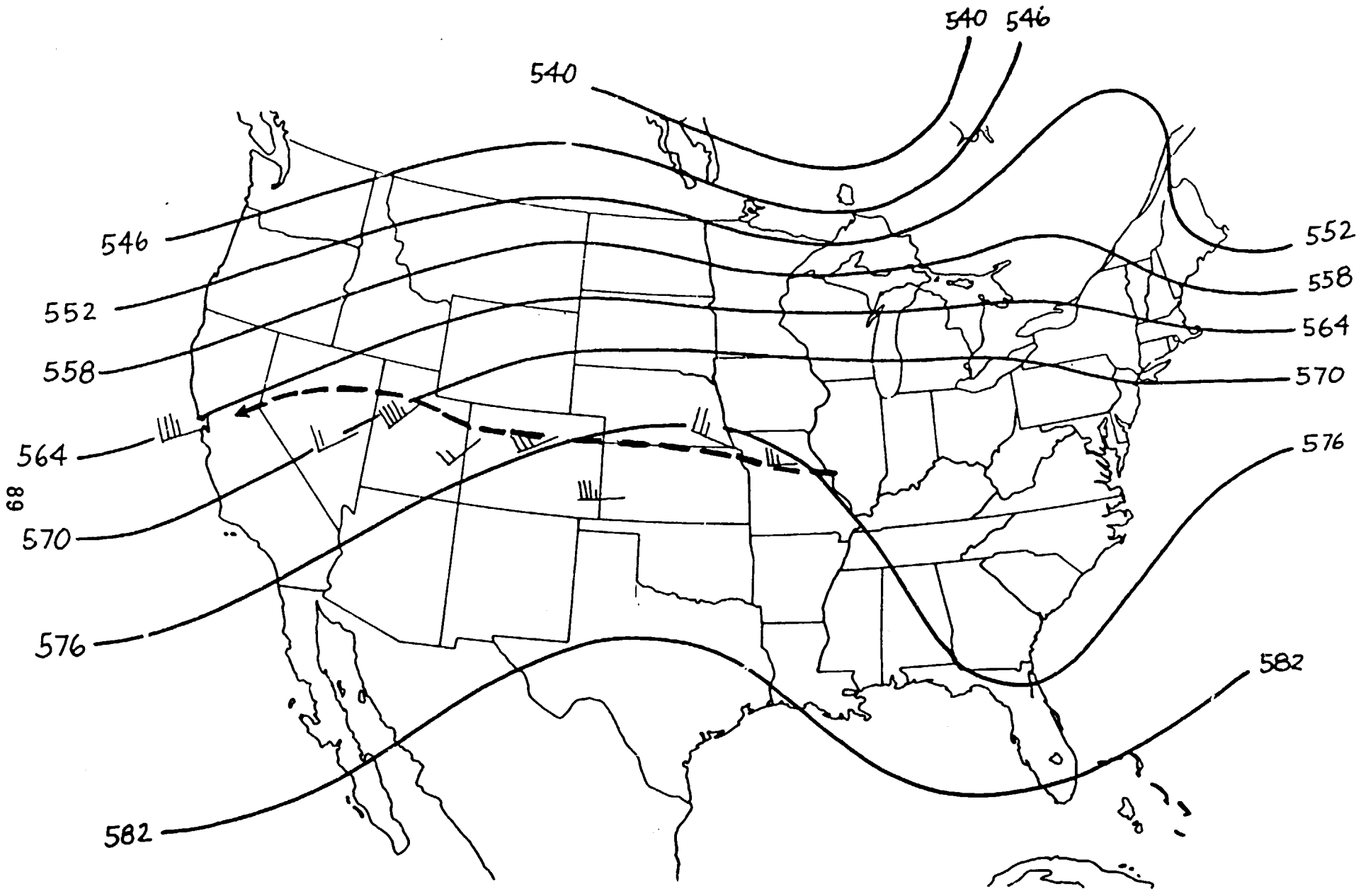

Figure 24b 500mb-May 4,0000z,1963

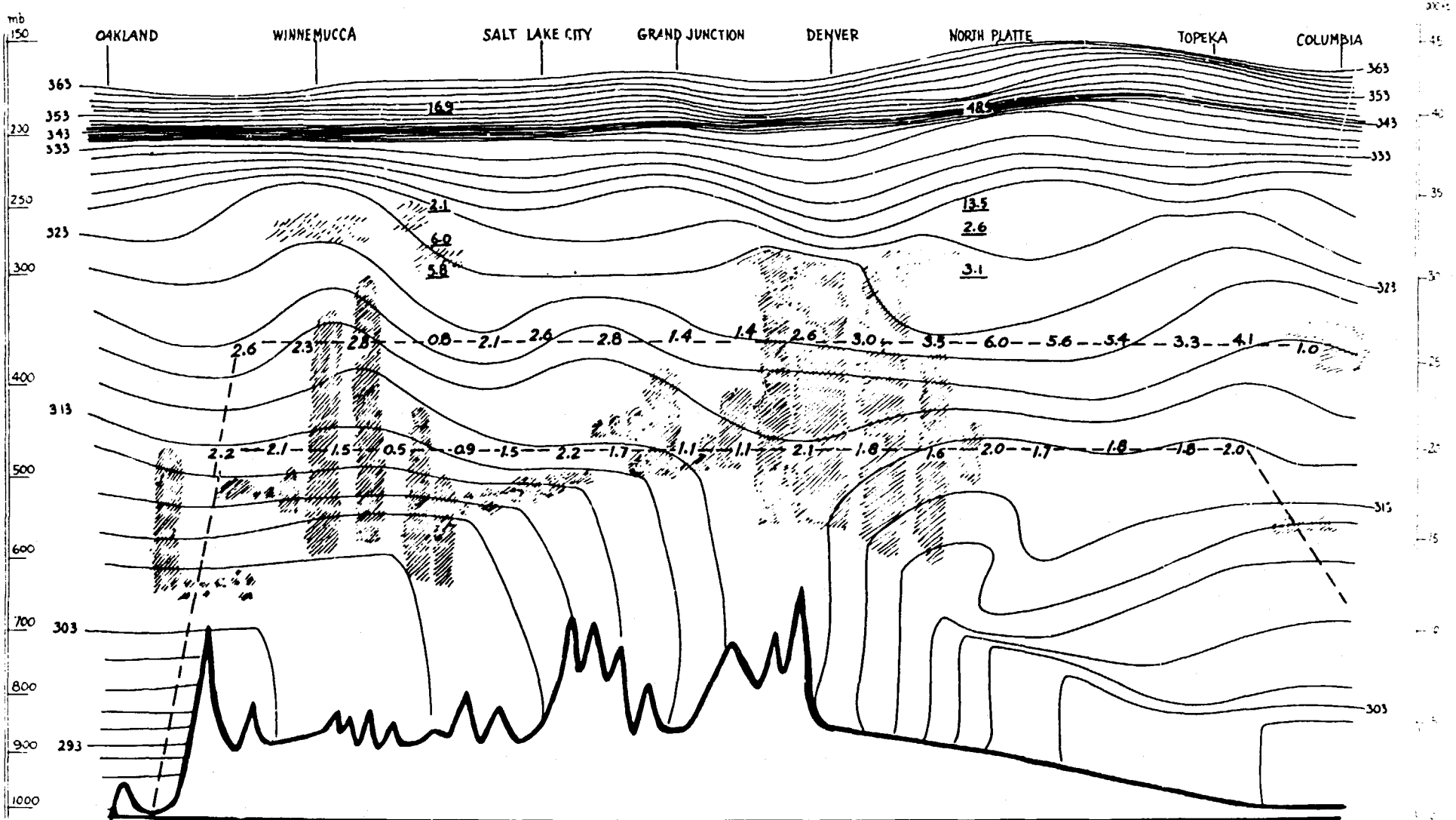

Vertical Cross Section for May 4, 1963, 0000z. Flight Paths shown by Dashed Lines.-Total β Activities of Filter Samples in dpm/SCF Plotted along Flight Paths.

Figure 25

RB-57's sampled at both locations at the times when the WB-50's passed below. Notice that the 5.8 and 6 dpm/SCF sampled west of Salt Lake were at the same Θ as the 6 and 5.6 dpm/SCF sampled east of North Platte by the WB-50 #2. Notice also that the activities were lower at the higher altitude in both places. The larger values may represent the diluted remnants of an extruded layer. It is interesting that the β activity did not increase with height in the upper troposphere, as is so often assumed. Even in the stratosphere a decrease with height is implied by the 48.5 dpm/SCF in the layer of very high stability and the 16.9 dpm/SCF sampled from above the layer.

The continuous radioactivity traces for the two WB-50's are shown in the lower diagram of Figure 26. Reproduced in the upper diagram is the trace for aircraft #2 from Figure 16. The contrast between the two May 3rd flights and the April 21st flight leaves little to be said about the importance of the stratospheric layers.

It is interesting, however, to note that although the 26,000 foot aircraft accumulated 1.8 times as much activity as the 20,000 foot aircraft (the same ratio as obtained by adding the β activities of the filters) the traces do not show a continual increase. The discrete filters would imply a non-uniform increase, but definitely an increase, while the traces show small steps followed by an almost level trace.

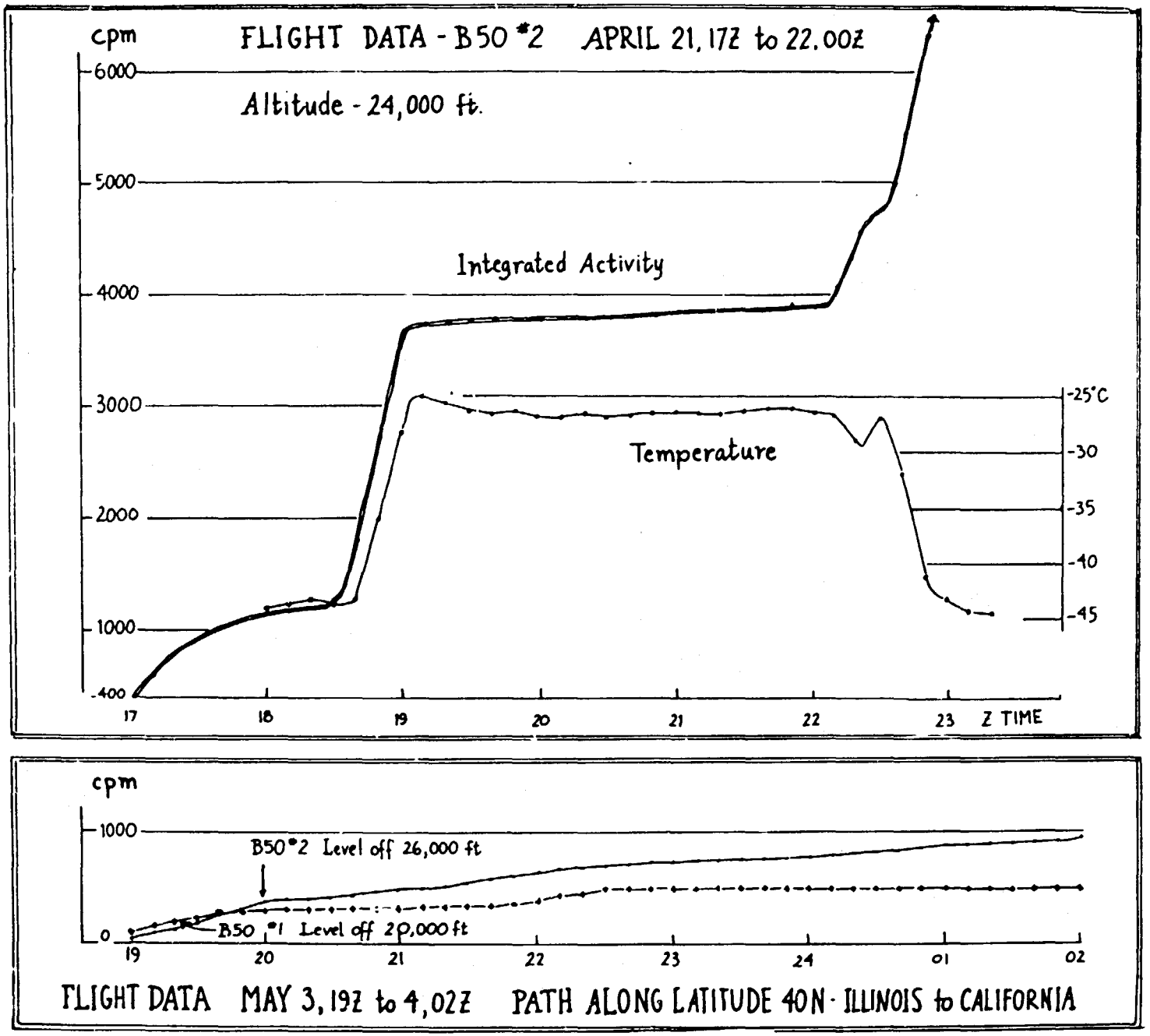
cpm
FLIGHT DATA - B50 #2 APRIL 21, 17Z to 22.00Z
6000
Altitude - 24,000 ft.
5000
Integrated Activity
4000
3000
Temperature
2000
1000
400
-25°C
-30
-35
-40
-45
17
18
19
20
21
22
23
Z TIME
cpm
1000
B50 #2 Level off 26,000 ft
B50 #1 Level off 20,000 ft
0
19
20
21
22
23
24
01
02
FLIGHT DATA MAY 3, 19Z to 4, 02Z PATH ALONG LATITUDE 40N - ILLINOIS to CALIFORNIA

Figure 26

The discrepancy was traced to the accumulation of radon daughter products which decay with a half life of about 20 minutes. The biggest steps occurred at 2200 Z when the planes reported light turbulence in the vicinity of the rain showers along the east slope of the Rocky Mountains. Notice the adiabatic lapse rates extended almost up to the 20,000 foot level in the Denver region.

Radon escaping from the earth was evidently carried aloft by the turbulent mixing in the adiabatic layer. The subsequent rapid decay of the radon daughters dominated the instantaneous counting rate but had little net effect on the total accumulation.

CHAPTER V

SUMMARY AND CONCLUSIONS

The radioactivity and meteorological observations obtained during Project SPRINGFIELD have established the validity of the tropopause folding proposed by Reed in 1955. The simultaneous increase in radioactivity, increase in temperature, increase in wind speed and decrease in dew point which was observed as the aircraft passed through the forecasted layers leaves little room for the skeptic about the folding process and the stratospheric properties of the air in the layer.

Of probably greater importance is the evidence in support of a positive correlation between the radioactivity and the potential vorticity. The correlations in these data were sufficiently consistent to warrant quantitative estimates of the radioactivity concentrations based on the potential vorticity calculations. Since the latter can be computed over the entire volume of the troposphere and much of the stratosphere, a reasonable distribution of radioactivity can be determined. Reasonable in the sense that it will show the layered structure of the radioactivity in both the troposphere and stratosphere. It will also show, as did the SPRINGFIELD data, that a layer in the middle troposphere may have a much higher concentration of radioactivity than exists in the stratosphere 20,000 or 30,000 feet above it.

The SPRINGFIELD data also supports the author's assumption that the large values of potential vorticity are created in the middle stratosphere and the low values in the lower troposphere. All samples from air with large values of potential vorticity contained high activities -- as yet there has been no exception, both in the SPRINGFIELD data and the 1960 data. This indicates that the stratospheric air moves diabatically down through the stratosphere on the cyclonic side of the jet. Then it is extruded from the lower stratosphere into the troposphere where it passes beneath the jet as it descends and moves to lower latitudes.

Project SPRINGFIELD provides the meteorologist with tangible evidence that adiabatic transports are significant and that they can be computed in three dimensions from the isentropic charts. During the past twenty years the isentropic charts have been neglected or ignored. As a consequence, the meteorologist has been conditioned to visualize the atmosphere from horizontal surfaces widely separated vertically. The flow patterns on the pressure surfaces mislead the meteorologist with respect to the actual three dimensional motions of the air parcels. The importance of stratospheric-tropospheric transport has been underestimated both in the process of cyclogenesis and in the production of severe weather.

Isentropic charts for the northern hemisphere are now available or can readily be prepared by machine methods. A. Gustafson of the United States Weather Bureau has developed and tested a program for computing the pressure, temperature, isentropic stream function and geostrophic potential vorticity by interpolating from the machine analysed isobaric charts. R. Duquet and the author, at Pennsylvania State University, have developed a program for calculating all of the isentropic data, including the winds and moisture by integrating each sounding from the surface to any specified upper level. Hemispheric charts are currently being produced and analysed. The data look good and the prospects for studying the three dimensional motions on a hemispheric scale are exciting. The significance of these motions to the problem of world-wide radioactive fallout can now be investigated.

REFERENCES

1. Bjerknes, J., and E. Palmen: Investigations of Selected European Cyclones by Means of Serial Ascents. Geofys. Publ. 12, No. 2 (1937).

2. Sawyer, J. S.: Day-to-Day Variations in the Tropopause. Geophys. Mem. No. 92, Vol. II, No. 7 (1954).

3. Reed, R. J.: A Study of a Characteristic Type of Upper Level Frontogenesis. J. Met. 12, (1955).

4. Reed, R., and E. F. Danielsen: Fronts in the Vicinity of the Tropopause. Arch. Met. Geoph. Biokl. A 11, 1 (1959).

5. Danielsen, E. F.: The Laminar Structure of the Atmosphere and Its Relation to the Concept of a Tropopause. Arch. Met. Geoph. Biokl. A 11, 3 (1959).

6. Danielsen, E. F.: Trajectories: Isobaric, Isentropic and Actual. J. Met. 18, 4 (1961).

7. Danielsen, E. F., and K. Bergman and C. Paulson: Radioisotopes, Potential Temperature and Potential Vorticity. University of Washington, Met. Dept. Report, (1962).

8. Junge, C. E., and J. Manson: Stratospheric Aerosol Studies. J. G. R., Vol. 66, No 7 (1961).

9. Friend, J. P., and R. D. Sherwood: The Size Distribution and Composition of Stratospheric Particles. Science, 133 (1961).

10. Bigg, E. K., and G. T. Miles: Stratospheric Ice Nucleus Measurements from Balloons. Tellus 15, No 2 (1963).

UNCLASSIFIED

Security Classification

DOCUMENT CONTROL DATA - R&D

(Security classification of title, body of abstract and indexing annotation must be entered when the overall report is classified)

1. ORIGINATING ACTIVITY (Corporate author) Defense Atomic Support Agency	2a. REPORT SECURITY CLASSIFICATION UNCLASSIFIED 2b. GROUP

3. REPORT TITLE

PROJECT SPRINGFIELD REPORT

4. DESCRIPTIVE NOTES (Type of report and inclusive dates)

Progress Report Spring 1963

5. AUTHOR(S) (Last name, first name, initial)

DANIELSEN, Edwin, F.

6. REPORT DATE	7a. TOTAL NO. OF PAGES	7b. NO. OF REFS
July 1964	103	10

8a. CONTRACT OR GRANT NO.	9a. ORIGINATOR'S REPORT NUMBER(S)
DA-49-146-XZ-079 b. PROJECT NO. c. d.	DASA 1517 9b. OTHER REPORT NO(S) (Any other numbers that may be assigned this report) NONE

10. AVAILABILITY/LIMITATION NOTICES

Qualified requestors may obtain this report from the Defense Documentation Center

11. SUPPLEMENTARY NOTES	12. SPONSORING MILITARY ACTIVITY
----------	Defense Atomic Support Agency

13. ABSTRACT

This report is concerned with the theory and confirmation of a stratospheric tropospheric exchange which accompanies a folding of the tropopause. Air from the lower part of the cyclonic stratosphere is extruded to form a thin inclined layer in the troposphere. The SPRINGFIELD data prove that the extruded tropospheric layers contain radioactivity concentrations typical of the stratosphere. Concentrations exceeding the tropospheric by one or two orders of magnitude were measured aboard WB-50 and RB-57 aircraft on specially vectored flight paths. The sharp change in concentrations at the boundaries also confirms that the folding process is predominately laminar, so it is appropriate to refer to the exchange as a transport rather than a diffusion process.

The agreement between the radioactivity and meteorological measurements is remarkable. Of particular value to the radiochemist and meteorologist is the high correlation between the concentrations of radioactivity and the potential vorticity. Since the latter can be determined from conventional radiosonde data, the three dimensional distribution of the former can be approximated. The distribution is not simple but the presence of the layers cannot be ignored in the fallout problem. Each layer acts as a low altitude source for both wet and dry fallout.

The report contains as complete a description of the folding and transport process as is possible to date. Physical processes capable of mixing the radioactivity from the layers to the ground are also discussed, including their probable distribution with respect to the extruded layers.

DD FORM 1 JAN 64 1473

UNCLASSIFIED

Security Classification

UNCLASSIFIED
Security Classification

14 KEY WORDS	LINK A		LINK B		LINK C	
	ROLE	WT	ROLE	WT	ROLE	WT
Springfield, Star Dust, HASP, World-Wide Fallout, Tropopause Folding, Radioactive Transfer, Precipitation, Ozone, Troposphere Mixing, Cyclogenesis, Sampling, Meteorology, Extruded Layers, Flight Paths, Radioactive Transport, Diffusion, Potential Vorticity, Radiosonde, Potential Temperature, Sr-90, Sr-89, W-185, Be-7						

INSTRUCTIONS

1. ORIGINATING ACTIVITY: Enter the name and address of the contractor, subcontractor, grantee, Department of Defense activity or other organization *(corporate author)* issuing the report.

2a. REPORT SECURITY CLASSIFICATION: Enter the overall security classification of the report. Indicate whether "Restricted Data" is included. Marking is to be in accordance with appropriate security regulations.

2b. GROUP: Automatic downgrading is specified in DoD Directive 5200.10 and Armed Forces Industrial Manual. Enter the group number. Also, when applicable, show that optional markings have been used for Group 3 and Group 4 as authorized.

3. REPORT TITLE: Enter the complete report title in all capital letters. Titles in all cases should be unclassified. If a meaningful title cannot be selected without classification, show title classification in all capitals in parenthesis immediately following the title.

4. DESCRIPTIVE NOTES: If appropriate, enter the type of report, e.g., interim, progress, summary, annual, or final. Give the inclusive dates when a specific reporting period is covered.

5. AUTHOR(S): Enter the name(s) of author(s) as shown on or in the report. Enter last name, first name, and middle initial. If military, show rank and branch of service. The name of the principal author is an absolute minimum requirement.

6. REPORT DATE: Enter the date of the report as day, month, year, or month, year. If more than one date appears on the report, use date of publication.

7a. TOTAL NUMBER OF PAGES: The total page count should follow normal pagination procedures, i.e., enter the number of pages containing information.

7b. NUMBER OF REFERENCES: Enter the total number of references cited in the report.

8a. CONTRACT OR GRANT NUMBER: If appropriate, enter the applicable number of the contract or grant under which the report was written.

8b, 8c, & 8d. PROJECT NUMBER: Enter the appropriate military department identification, such as project number, subproject number, system numbers, task number, etc.

9a. ORIGINATOR'S REPORT NUMBER(S): Enter the official report number by which the document will be identified and controlled by the originating activity. This number must be unique to this report.

9b. OTHER REPORT NUMBER(S): If the report has been assigned any other report numbers *(either by the originator or by the sponsor)*, also enter this number(s).

10. AVAILABILITY/LIMITATION NOTICES: Enter any limitations on further dissemination of the report, other than those imposed by security classification, using standard statements such as:

(1) "Qualified requesters may obtain copies of this report from DDC."

(2) "Foreign announcement and dissemination of this report by DDC is not authorized."

(3) "U. S. Government agencies may obtain copies of this report directly from DDC. Other qualified DDC users shall request through _____."

(4) "U. S. military agencies may obtain copies of this report directly from DDC. Other qualified users shall request through _____."

(5) "All distribution of this report is controlled. Qualified DDC users shall request through _____."

If the report has been furnished to the Office of Technical Services, Department of Commerce, for sale to the public, indicate this fact and enter the price, if known.

11. SUPPLEMENTARY NOTES: Use for additional explanatory notes.

12. SPONSORING MILITARY ACTIVITY: Enter the name of the departmental project office or laboratory sponsoring *(paying for)* the research and development. Include address.

13. ABSTRACT: Enter an abstract giving a brief and factual summary of the document indicative of the report, even though it may also appear elsewhere in the body of the technical report. If additional space is required, a continuation sheet shall be attached.

It is highly desirable that the abstract of classified reports be unclassified. Each paragraph of the abstract shall end with an indication of the military security classification of the information in the paragraph, represented as *(TS), (S), (C), or (U)*.

There is no limitation on the length of the abstract. However, the suggested length is from 150 to 225 words.

14. KEY WORDS: Key words are technically meaningful terms or short phrases that characterize a report and may be used as index entries for cataloging the report. Key words must be selected so that no security classification is required. Identifiers, such as equipment model designation, trade name, military project code name, geographic location, may be used as key words but will be followed by an indication of technical context. The assignment of links, rules, and weights is optional.

UNCLASSIFIED
Security Classification